

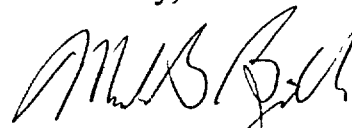
Mark B. Bezilla
Site Vice President724-682-5234
Fax. 724-643-8069April 4, 2003
L-03-064U. S. Nuclear Regulatory Commission
Attention: Document Control Desk
Washington, DC 20555-0001**Subject: Beaver Valley Power Station, Unit No. 1 and No. 2
BV-1 Docket No. 50-334, License No. DPR-66
BV-2 Docket No. 50-412, License No. NPF-73
Supplemental Information Supporting Proposed Alternative Repair
Methods for Reactor Vessel Head Penetrations (Relief Request No.
BV3-RV-04)**

On March 28, 2003, the FirstEnergy Nuclear Operating Company (FENOC) submitted a relief request for approval of a reactor vessel head penetration alternative repair method (embedded flaw repair). In the submittal, FENOC submitted Relief Request BV3-RV-04 to the requirements of Section XI of the ASME Code requesting authorization to use the embedded flaw repair technique.

On April 3, 2003, the FirstEnergy Nuclear Operating Company (FENOC) submitted a response to a request for additional information on the subject relief request which referenced WCAP 15986 "The Embedded Flaw Process for Repair of Reactor Vessel Head Penetrations and Its Application at North Anna Unit 2" dated March 2003. This WCAP is being provided as an attachment to this submittal in order to docket the information.

No new commitments are contained in this submittal. If there are any questions regarding this matter, please contact Mr. Larry R. Freeland, Manager, Regulatory Affairs/Performance Improvement at 724-682-5284.

Sincerely,



Mark B. Bezilla

Enclosure

A047

Beaver Valley Power Station, Unit No. 1 and 2
Supplemental Information Supporting Proposed Alternative Repair Methods for Reactor
Vessel Head Penetrations (Relief Request No. BV3-RV-04)
L-03-064
Page 2

c: Mr. T. G. Colburn, NRR Senior Project Manager
Mr. D. M. Kern, NRC Sr. Resident Inspector
Mr. H. J. Miller, NRC Region I Administrator

Westinghouse Proprietary Class 3

WCAP-15986

March 2003

The Embedded Flaw Process for Repair of Reactor Vessel Head Penetrations and Its Application at North Anna Unit 2

WCAP-15986

The Embedded Flaw Process for Repair of Reactor Vessel Head Penetrations and Its Application at North Anna Unit 2

**W. H. Bamford
J. P. Lareau
J. F. Duran
R. E. Gold
P. K. Evans
W. R. Gahwiller**

March 2003

Reviewer: _____
Di Tang
Structural Mechanics Technology

Approved: _____
E. A. Siegel, Manager
Alloy 600 Product Line

Westinghouse Electric Company LLC
P.O. Box 355
Pittsburgh, PA 15230-0355

© 2003 Westinghouse Electric Company LLC
All Rights Reserved

TABLE OF CONTENTS

1	BACKGROUND AND INTRODUCTION.....	1-1
1.1	Summary of Technical Basis for the Embedded Flaw Repair.....	1-1
1.2	Discussion of Geometry and Manufacturing Details.....	1-2
1.3	Qualification of the Embedded Flaw Repair Process.....	1-3
2	RECENT FINDINGS AT NORTH ANNA UNIT 2: SEPTEMBER 2002.....	2-1
2.1	Visual Examination Results: Head Outer Surface.....	2-1
2.2	Liquid Penetrant Exam Results.....	2-1
2.3	Inner Periphery of the Repair Weld.....	2-1
2.4	Within the Repair Weld Itself.....	2-1
2.5	On the Periphery of the Repair Weld.....	2-2
2.6	Examination Results on the Penetration Tube Inner Diameter.....	2-2
3	RESOLUTION OF INDICATIONS IN AND NEAR THE EMBEDDED FLAW REPAIR WELD.....	3-1
4	BACKGROUND AND EXPERIENCE – SCC RESISTANCE OF ALLOY 52.....	4-1
4.1	Introduction.....	4-1
4.2	Service Experience.....	4-2
4.3	Laboratory Experience.....	4-3
5	REVISIONS TO THE EMBEDDED FLAW REPAIR PROCESS.....	5-1
6	SUMMARY AND CONCLUSIONS.....	6-1
7	REFERENCES.....	7-1
	APPENDIX A BASIS FOR SELECTION OF ALLOY 690 FOR STEAM GENERATOR HEAT TRANSFER TUBING.....	A-1
	APPENDIX B METALLURGICAL EVALUATION OF AN EMBEDDED FLAW REPAIR SAMPLE REMOVED FROM THE NORTH ANNA UNIT 2 RPV HEAD.....	B-1

1 BACKGROUND AND INTRODUCTION

During the fall 2002 outage at North Anna Unit 2, a number of indications were discovered in the attachment welds for the reactor vessel head penetrations. Indications were also found in three penetrations that had been repaired during the fall outage of 2001. The objective of this report is to provide the details of those inspections and their resolution.

Some of these findings have called into question the viability of the repairs completed in the fall of 2001. This report will also review the technical basis of the embedded flaw repair methodology, and discuss the implications of the recent findings.

It was concluded that the indications in the repair welds are the result of two different causes. The first was the surface flapping that was done prior to the recent penetrant exams, exposing a number of small indications, both rounded and linear. These have been removed by grinding, and were not an integrity concern, even if they had been left there. The second source of the indications was the Alloy 182 buttering which was not completely covered by the weld repair. This was an application process error, which is being corrected.

These findings lead to the conclusion that the embedded flaw weld repair process is an acceptable process when properly applied to cover the entire J-groove weld and buttering.

1.1 SUMMARY OF TECHNICAL BASIS FOR THE EMBEDDED FLAW REPAIR

The embedded flaw repair technique was developed by Westinghouse in 1994, and involves the deposition of at least two layers of Alloy 52 weld metal to isolate existing flaws and susceptible material from the primary water environment.

The embedded flaw repair technique is considered a permanent repair for the following reasons: first, as long as a Primary Water Stress Corrosion Crack (PWSCC) remains isolated from the primary water (PW) environment, it cannot propagate. Since Alloy 52 weldment is highly resistant to PWSCC, a new PWSCC crack will not initiate and grow through the Alloy 52 overlay to permit the PW environment to contact the susceptible material. The resistance of Alloy 690 and its associated welds, Alloys 52 and 152, has been demonstrated by laboratory testing in which no cracking has been observed in simulated PWR environments, and by approximately 10 years of operational service in steam generator tubes, where no PWSCC has occurred. The crack growth resistance of this material has been documented in EPRI Report TR-109136, "Crack Growth and Microstructural Characterization of Alloy 600 PWR Vessel Head Penetration Materials," [1] and other papers. The service experience will be further discussed in Section 4.

The residual stresses produced by the embedded flaw technique have been measured and found to be relatively low [2] because of the small thickness of the weld. This implies that no new cracks will initiate and grow in the area adjacent to the repair weld. There are no other known mechanisms for significant crack propagation in this region because the cyclic fatigue loading is considered negligible. Cumulative Usage Factor (CUF) in the upper head region was calculated to be less than 0.2 [3] in the reactor vessel design report, as well as in various aging management review reports.

The thermal expansion properties of Alloy 52 weld metal are not specified in the ASME code, as is the case for other weld metals. In this case, the properties of the equivalent base metal (Alloy 690) should be used. For that material, the thermal expansion coefficient at 600°F is 8.2 E-6 in/in/degree F as found in Section II Part D. The Alloy 600 base metal has a coefficient of thermal expansion of 7.8 E-6 in/in/degree F, a difference of about 5 percent.

The effect of this small difference in thermal expansion is that the weld metal will contract more than the base metal when it cools, thus producing a compressive stress on the Alloy 600 tube or the attachment weld, where the crack may be located. This beneficial effect has already been accounted for in the residual stress measurements reported in the technical basis for the embedded flaw repair.

The small residual stress produced by the embedded flaw weld will act constantly, and therefore, will have no impact on the fatigue effects in the CRDM region. Since the stress would be additive to the maximum as well as the minimum stress, the stress range would not change, and the already negligible usage factor, noted above, for the region would not change at all.

1.2 DISCUSSION OF GEOMETRY AND MANUFACTURING DETAILS

Fabrication of the North Anna Unit 2 closure head was performed by Rotterdam Dockyard Company. The closure head is clad with austenitic stainless steel. Cladding thickness is a minimum of 3.2 mm and a nominal 4 mm. The J-groove weld cavity was prepared manually. The J-groove weld cavity was buttered by manual shielded metal arc welding using a coated electrode according to ASME SB-295 ENiCrFe-3 (Alloy 182) [5]. The penetration was welded to the closure head using either a combination of manual gas tungsten arc and manual gas metal arc welding (Alloy 82) [4] or shielded metal arc welding with Alloy 182.

The geometry of the J-groove cavity and buttering is shown in Figures 1-1 through 1-7. These figures are based on Rotterdam drawings 30660-1088 [6], and 30660-1097 [7]. They provide the nominal and the minimum and maximum dimensions of the J-groove and buttering, based on varying the depth of the J-groove and the thickness of the buttering. Figures are provided for penetration 51 and penetrations 62 and 63. These figures provide the linear dimensions, expressed in millimeters, for the J-grooves and buttering. The tables below summarize the information on these sketches and the dimensions have been converted to inches.

Drawing 30660-1103 [8] does not indicate the J-groove welding extending beyond the buttering. However, the welding procedure, while not including a requirement for this, does include a figure indicating that the J-groove weld may extend beyond the buttering. If, during the manufacturing process, the J-groove welding did extend beyond the buttering, the actual area of Alloy 82/182-weld metal may be larger than shown on the figures.

These dimensions help to identify the nominal, minimum, and maximum sizes of the welds on the penetrations, which were repaired in the fall of 2001. The values were based on the tolerances provided in the drawing. In some cases, only single values were provided, and these were taken as nominal values and used throughout.

Figure 1-2 provides the nominal dimensions for penetration 51, showing that the buttering is much wider on the downhill side of the weld, than on the uphill side. This is because of the angular nature of the weld preparation, as well as the curvature of the head. From Figures 1-3 and 1-4 (penetration 51), we see that the width of the buttering on the downhill side can range from 12.7 to 34.8 millimeters. The results for penetrations 62 and 63 show the weld sizes are slightly larger, as seen in Figures 1-5 through 1-7.

1.3 QUALIFICATION OF THE EMBEDDED FLAW REPAIR PROCESS

In preparation for the Alloy 600 Repair Program, PCI Energy Services, a subsidiary of Westinghouse Electric, developed Procedure Qualification (PQR) # 695 which supports Welding Procedure Specification (WPS) WPS 3-43/F43-B MC-GTAW. This qualification consisted of a P3, Gr. 3 plate, buttered (1/8") with ERNiCrFe-7 (Alloy 52) and postweld heat-treated to 1200°F for 40 hrs. Joint dimensions were then machined onto the plate and it was fit-up to a SB-166, Alloy 600 plate with a backing strip. The joint was then welded out in the 3G position. Testing per ASME Section IX was performed (tensiles, bends and hardness tests) and PQR 695, was found to meet all acceptance criteria.

A second Procedure Qualification PQR 694A also supports WPS 3-43/F43-B MC-GTAW and WPS 3-43/52-TB MC-GTAW-N638, which is a combined "Temper Bead" weld and a 1/4 inch stainless steel (A8) overlay embedded at the top of the qualification coupon. As the "Temper Bead" weld was completed, the balance of the groove weld utilizing ERNiCrFe-7 (Alloy 52) was stepped out over and tied into the top of the stainless steel cladding. The non-temper bead portion of PQR 694A, was tested with bends and tensile tests, that included weld metal of the stainless steel clad and the Alloy 52 filler metal per ASME Section IX (QW-217). These tests permit the use of this weld to be used as a structural weld or as a weld overlay, concurrently. The "Temper Bead" portion of that qualification has been superseded by PQR 707, which is a moot point for the position Westinghouse is seeking to establish. This WPS is used primarily for overlay or weld build-up of the wetted surface after the "Temper Bead" technique has been utilized or if the utility chooses to perform and use the "Embedded Flaw Technique."

In parallel to the procedure development, welding equipment is designed, developed and certified by PCI Engineering. This equipment is tested at Lake Bluff, from 80 to 120 hours or more, to work out any bugs in the equipment and make sure the design works. If need be, at this stage, the tool is redesigned until it will perform the job it is intended for and it is certified with the customer approval.

Once the WPS is qualified and the equipment certified, the welders are brought into PCI, Lake Bluff to certify on the equipment. The welders are already qualified to weld Machine GTAW prior to starting this certification; however, this certification is over and above Code requirements. The welders spend an average of 220 hours to upwards of 280 hours to certify on the equipment.

Table 1-1 Distances from the Penetration Tube to the Extremity of the Weld Regions – North Anna Unit 2				
Penetration Number 51				
	High Side of Weld		Low Side of Weld	
	OD J-groove	OD Battering	OD J-groove	OD Battering
Nominal	17.6 mm (0.69 in.)	27.7 mm (1.09 in.)	34.9 mm (1.37 in.)	55.1 mm (2.17 in.)
Minimum Exposed Battering	21.4 mm (0.84 in.)	27.7 mm (1.09 in.)	42.5 mm (1.67 in.)	55.1 mm (2.17 in.)
Maximum Exposed Battering	13.2 mm (0.52 in.)	30.5 mm (1.20 in.)	26 0 mm (1.02 in.)	60.7 mm (2.39 in.)
Penetration Numbers 62 and 63				
	High Side of Weld		Low Side of Weld	
	OD J-groove	OD Battering	OD J-groove	OD Battering
Nominal	18.4 mm (0.72 in.)	29.2 mm (1.15 in.)	41.3 mm (1.63 in.)	66 5 mm (2.62 in.)
Minimum Exposed Battering	22.9 mm (0.90 in.)	29.2 mm (1.15 in.)	51.5 mm (2.03 in.)	66.3 mm (2.61 in.)
Maximum Exposed Battering	14.7 mm (0.58 in.)	32.3 mm (1.27 in.)	32.7 mm (1.29 in.)	73.4 mm (2.89 in.)

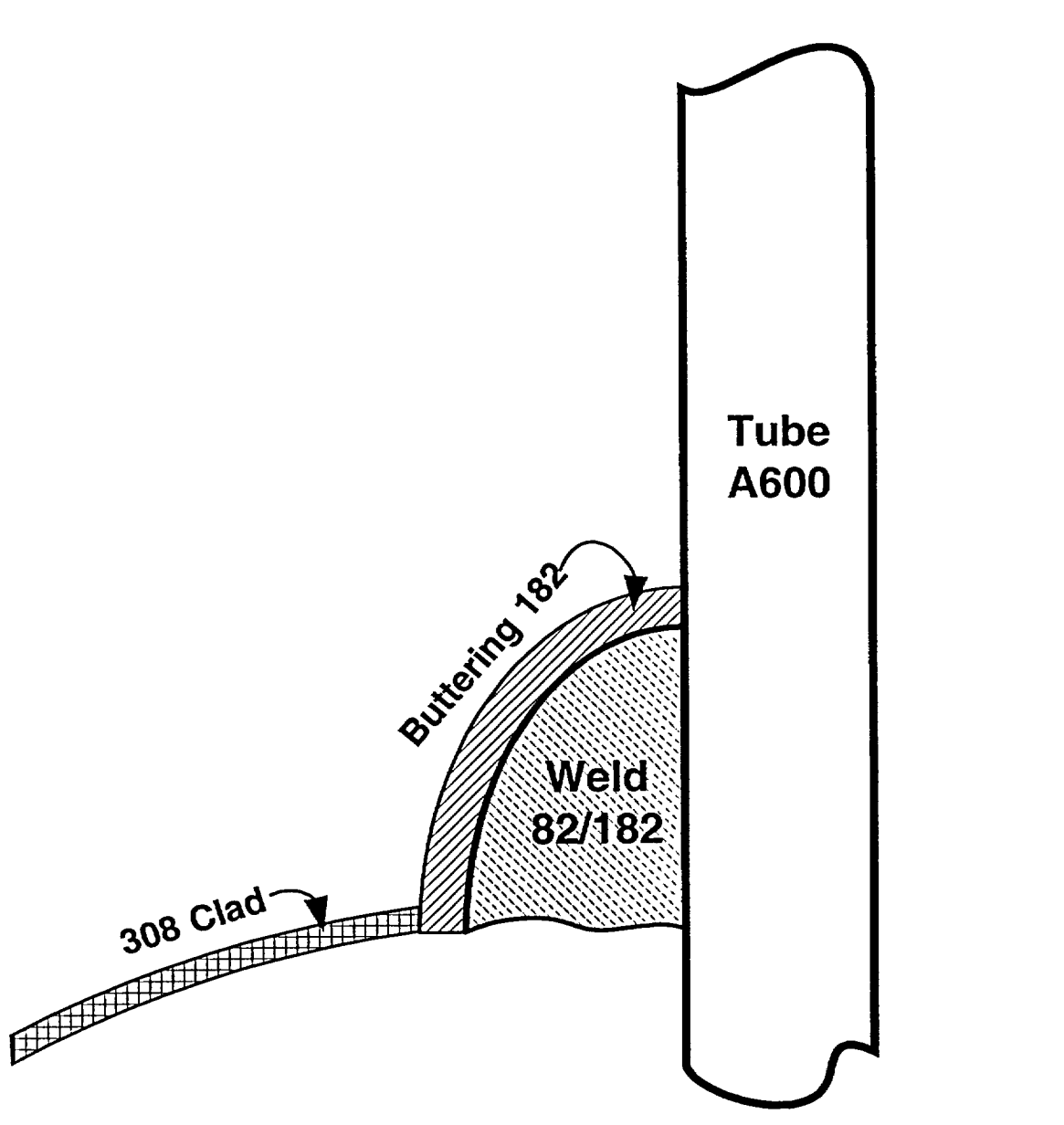


Figure 1-1 As-Built Configuration

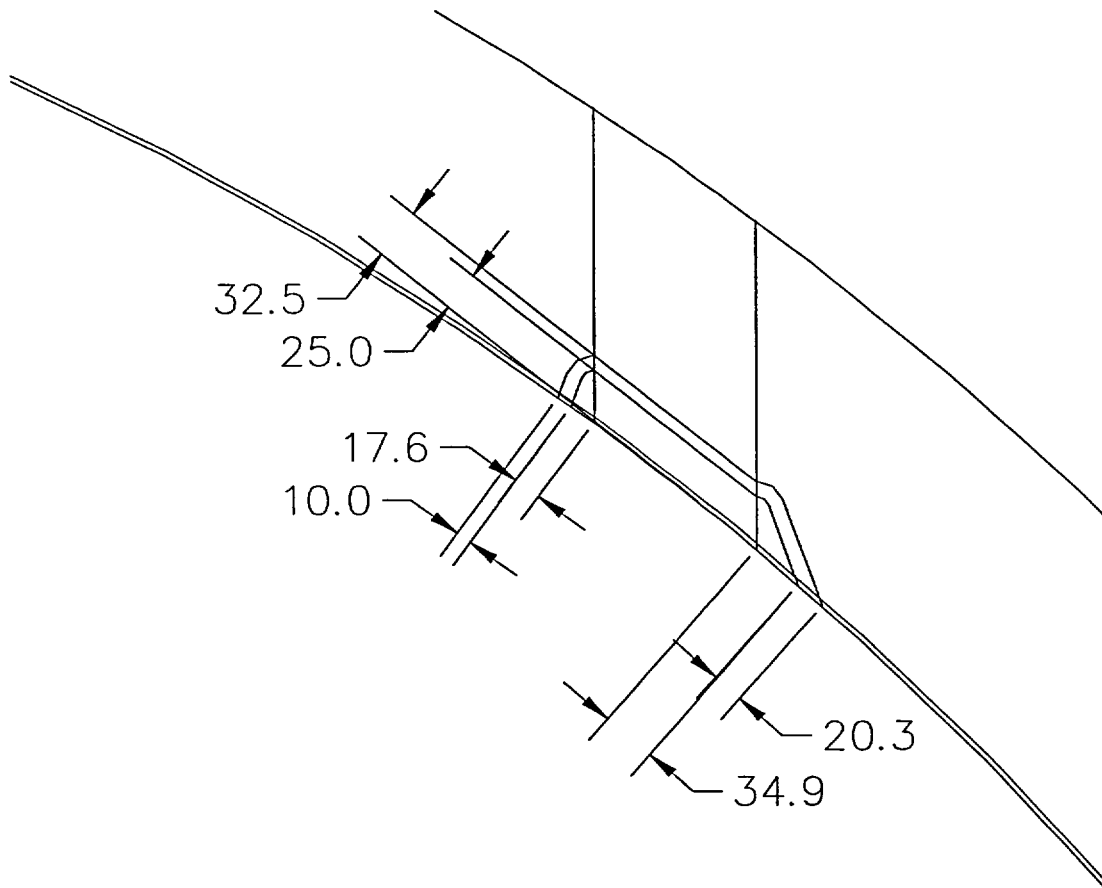


Figure 1-2 Penetration Number 51 Nominal J-Groove Dimensions in Millimeters

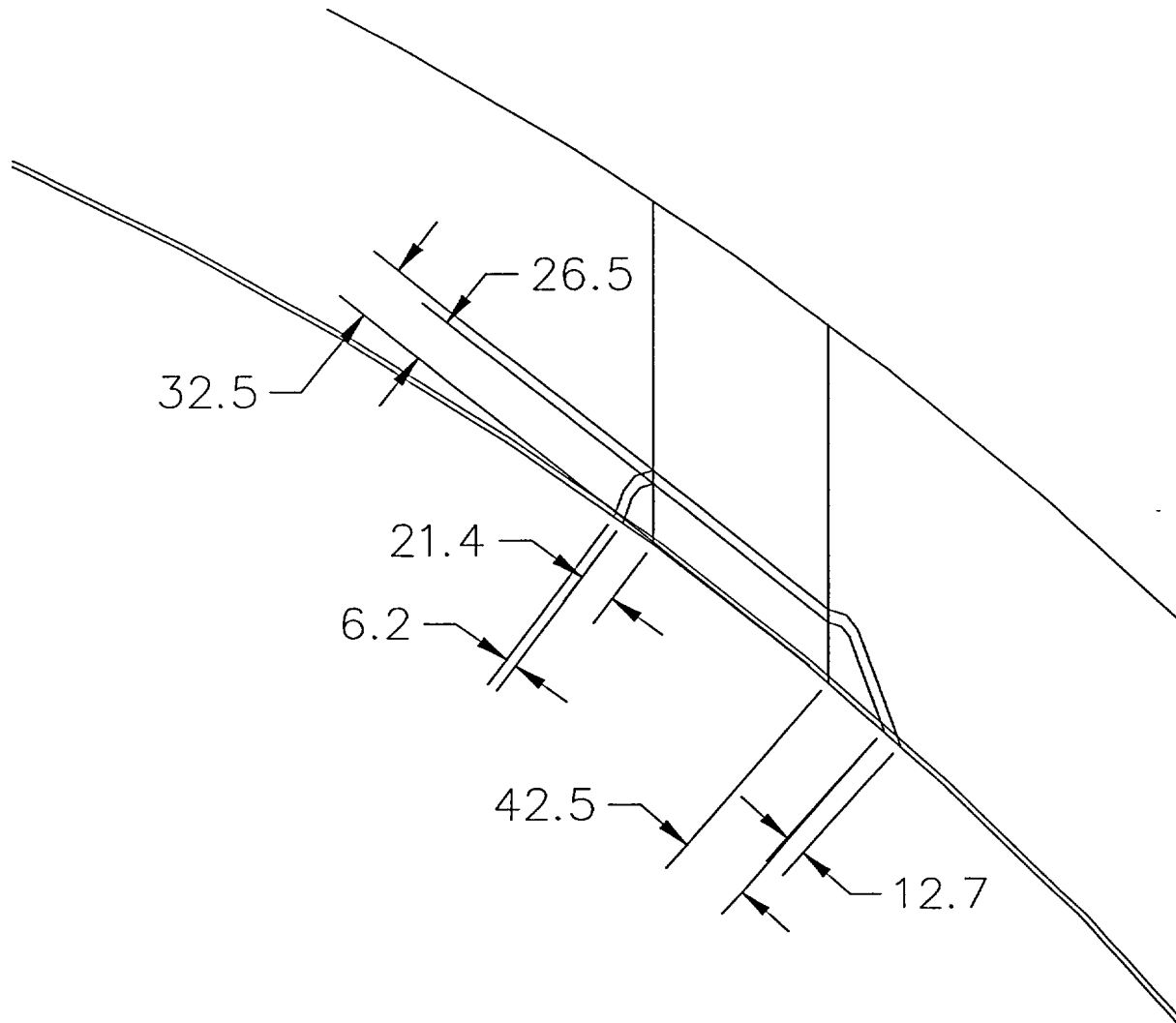


Figure 1-3 Penetration Number 51 Minimum J-Groove Dimensions in Millimeters

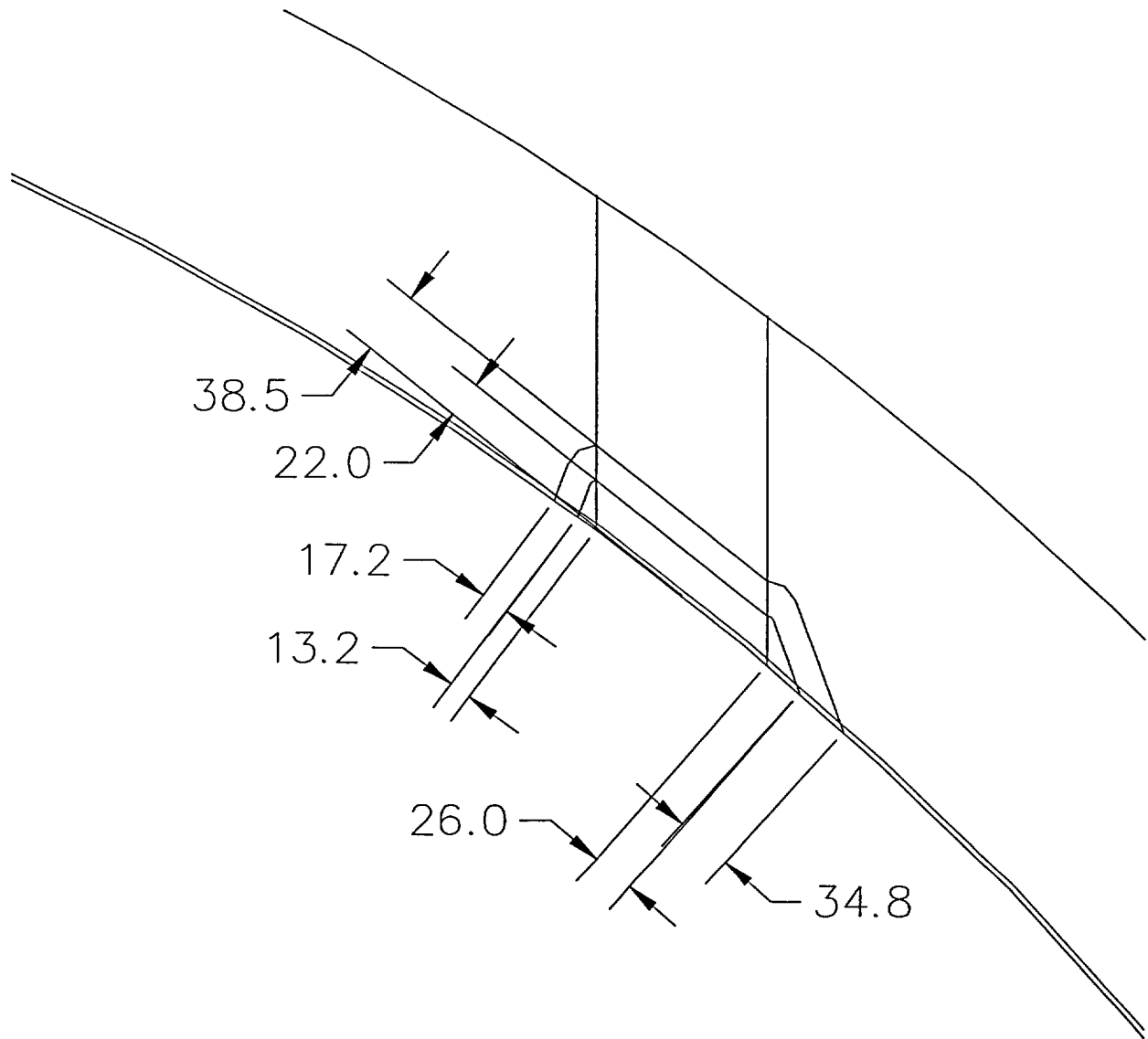


Figure 1-4 Penetration Number 51 Maximum J-Groove Dimensions in Millimeters

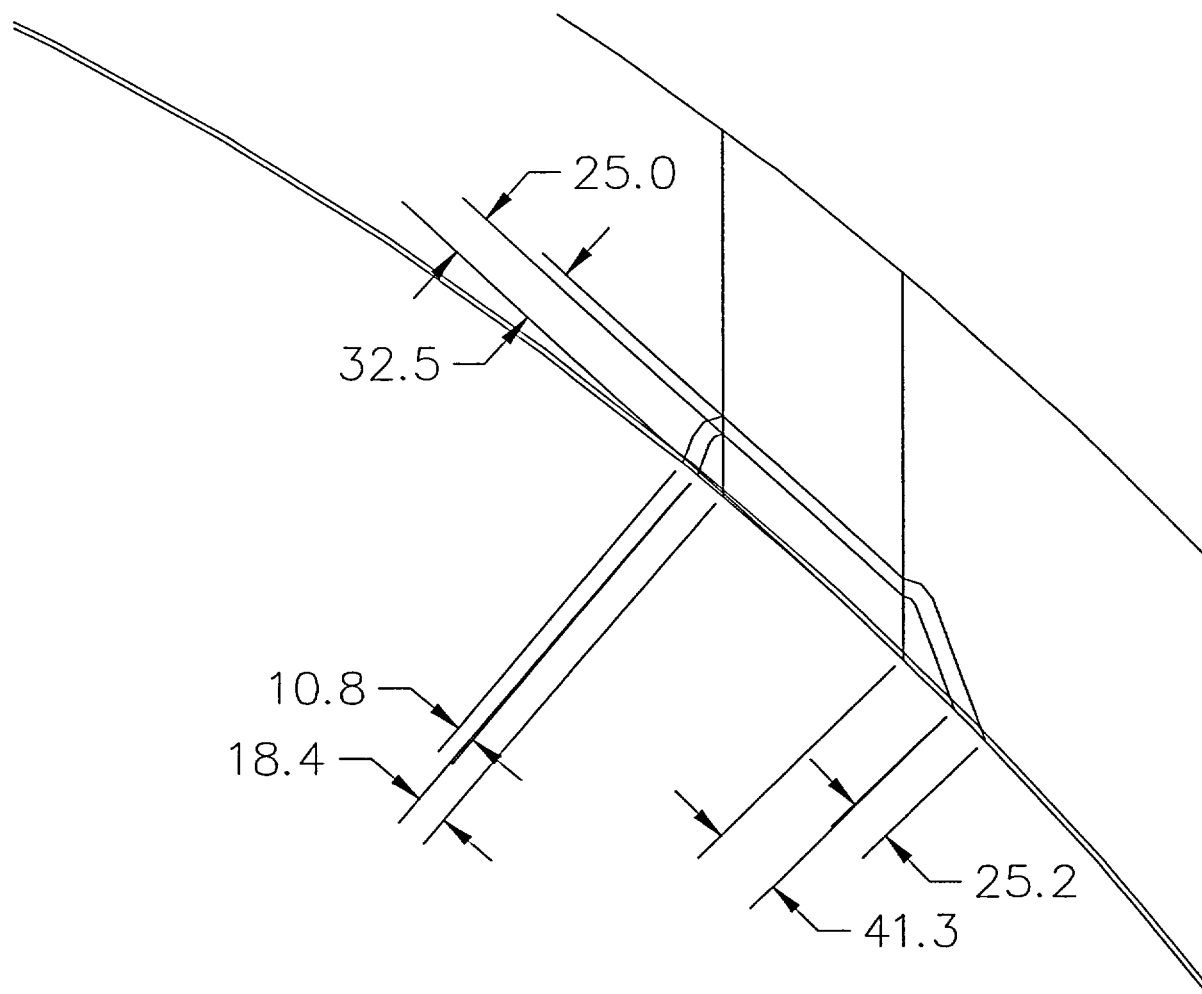


Figure 1-5 Penetration Numbers 62 and 63 Nominal J-Groove Dimensions in Millimeters

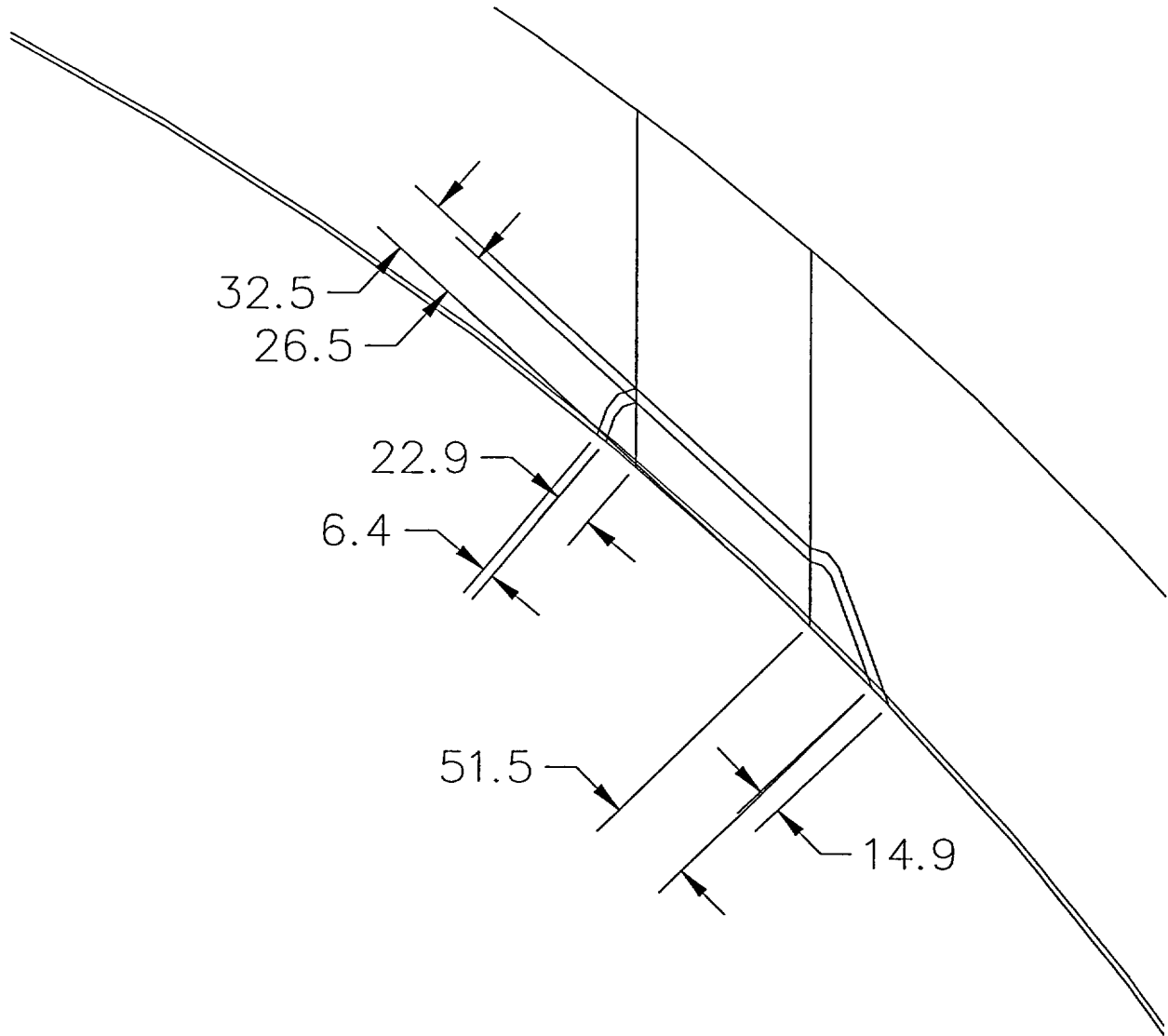


Figure 1-6 Penetration Numbers 62 and 63 Minimum J-Groove Dimensions in Millimeters

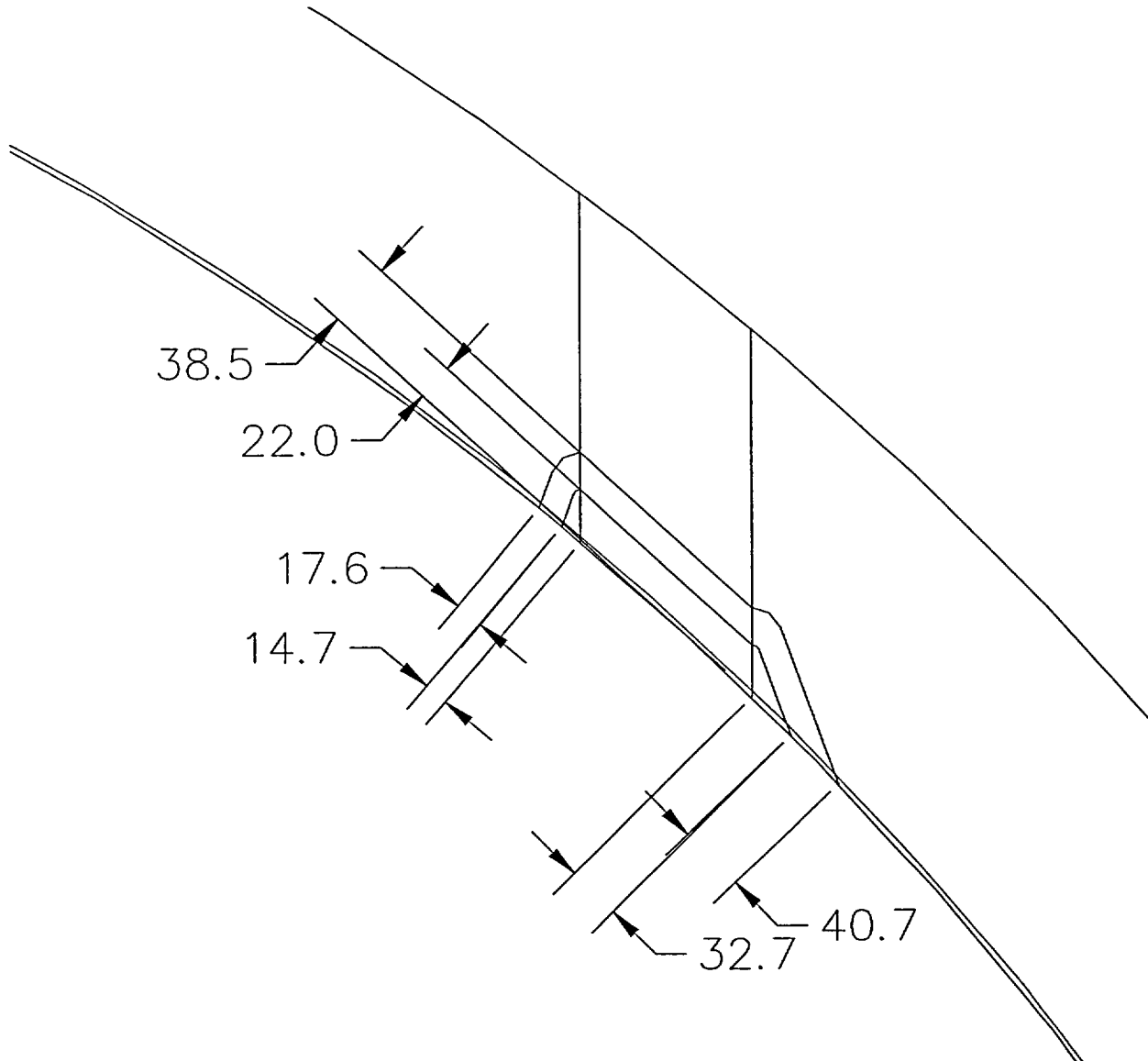


Figure 1-7 Penetration Numbers 62 and 63 Maximum J-Groove Dimensions in Millimeters

2 RECENT FINDINGS AT NORTH ANNA UNIT 2: SEPTEMBER 2002

2.1 VISUAL EXAMINATION RESULTS: HEAD OUTER SURFACE

The September 2002 examination of the reactor vessel head penetrations at North Anna Unit 2 began with a visual examination of the outer surface of the head, under the insulation. This visual exam revealed two penetrations (numbers 21 and 31), with "popcorn" (deposits of anhydrous boric acid) around the tubes, which is a strong indication of leakage. In addition, four penetrations (10, 35, 51, 57), were found with discernible boron deposits, and these were listed as probable leaking penetrations. Another 21 penetrations were masked by boric acid deposits on the head. After removal of the boric acid, the head was carefully re-inspected visually to determine if any boric acid corrosion had taken place, and no damage was found.

2.2 LIQUID PENETRANT EXAM RESULTS

As part of the inspection process, the three penetrations that had been previously repaired in the fall of 2001 (51, 62, and 63) were re-examined by liquid penetrant. Note that these locations had been dye penetrant inspected after the repairs at the last outage, and had been found to be free of indications. Prior to the application of the penetrant during the current outage, the region was, in each case, conditioned by application of a flapper wheel. All three penetrations showed indications as a result of the liquid penetrant examination. One of these penetrations, number 51, had also shown evidence of probable leakage on the outside surface of the head.

The indications are summarized in Table 2-1, and will be discussed in some detail here. The discussion will be focused on three regions, the inner periphery of the repair weld, the weld repair itself, and the outer periphery of the repair weld. In all cases, the circumferential location of the indication will be presented in terms of its angular location counter-clockwise from the bottom of the tube, noted as zero degrees. The viewing direction is from the underside of the head.

2.3 INNER PERIPHERY OF THE REPAIR WELD

Four penetrant indications were found at the inner toe of the repair weld, at the boundary with the penetration tube. This configuration is shown in Figure 2-1, and labeled "corner trap for PT." The weld boundary was not completely blended at this location. This left some sharp corners, which retained penetrant. This type of indication was found on penetrations 62 and 63. As noted in Section 2.2, this region was also conditioned with a flapper wheel, which may have led to the indications. All four of these indications were characterized as linear, and all were concluded to be non-relevant indications due to geometric discontinuities.

2.4 WITHIN THE REPAIR WELD ITSELF

Seven rounded indications and one very faint, fairly wide linear indication (near the outer periphery of the weld), were found in the weld itself. Located in all three penetrations, these indications are of no concern to the integrity of the weld, since none were crack-like. Their dye penetrant dimensions ranged from 0.10 to 0.75 inches, which made some of them unacceptable to the penetrant exam criteria.

The weld was PT-clear after the repair in fall 2001, and it is concluded that these indications were uncovered by the flapping process, prior to the recent PT.

Subsequent flapping and grinding with additional dye penetrant exams showed additional rounded indications. This sequence of findings indicates that subsurface, rather than surface-breaking flaws, were found in the repair welds.

2.5 ON THE PERIPHERY OF THE REPAIR WELD

Eight indications were found on the outer periphery of the repair weld, five in penetration 51, one in penetration 62, and two in penetration 63. The results of the initial liquid penetrant exams of penetration 51 are shown in Figures 2-2 and 2-3. Because of their location, additional work has been done to determine their cause, as will be discussed in Section 3.

2.6 EXAMINATION RESULTS ON THE PENETRATION TUBE INNER DIAMETER

The inside surface of the three penetration tubes was inspected in the fall of 2001 using both volumetric and surface examination methods, and these inspections are being repeated in the fall of 2002. At this time, the reinspection has only been completed on penetration 51. The results from both inspections are compared in Table 2-2.

Note that only the lengths of the indications have been characterized, and there is essentially no change. The fact that some of the indications seemed to get shorter is a measure of the scatter in the eddy current process. The depths were not measured by UT in 2002, but since these flaws were all very shallow, no growth is expected in depth.

Penetration/ Indication No.	Location (Degrees)	Position	Original Length	Description	Comments
51-1	190	Outer Periphery	0.31"	Linear	Blended, reduced length to 0.0625
51-2	135	Outer Periphery	0.125"	Linear	Boat sample
51-3	135	Outer Periphery	0.125"	Linear	Boat sample
51-4	125	Outer Periphery	0.10"	Rounded	
51-5	30	In Weld	0.25"	Rounded	
51-6	240	In Weld	0.25"	Rounded	Blended to remove, depth ≤ 0.1875 "
51-7	240	Outer Periphery	0.09"	Rounded	Blended to remove, depth ≤ 0.125 "
62-1	10	Inner Toe	2.5"	Linear	Blended to remove, depth ≤ 0.125
62-2	240	Inner Toe	2.25"	Linear	Blended to remove, depth ≤ 0.125
62-3	260	In Weld	0.375"	Rounded	Removed, ground to depth ≤ 0.0625
62-4	280	In Weld	0.375"	Rounded	Removed, ground to depth ≤ 0.0625
62-5	330	Outer Periphery	3.0"	Linear	
63-1	5	In Weld	0.75"	Rounded	Removed, ground to depth ≤ 0.0625
63-2	60	In Weld	0.75"	Rounded	Removed, ground to depth ≤ 0.0625
63-3	100	Outer Periphery	1.0"	Linear	
63-4	135	Inner Toe	0.10"	Linear	Blended to remove, depth ≤ 0.0625
63-5	160	Outer Periphery	0.10"	Linear	
63-6	270	Inner Toe	2.00"	Linear	Blended to remove, depth ≤ 0.0625
63-7	315	In Weld	0.75"	Rounded	Removed, Ground to depth ≤ 0.0625

Note: Indications 51-1, 51-6, and 51-7 were the only indications found in the original PT of 2002. All other indications were uncovered by subsequent grinding.

Table 2-2 Penetration #51 ID NDE Results							
Indication	2002 ECT Examination Results			2001 Examination Results			
	Circumference	Height	Length	Circumference	Height	Length	Depth
1	73°	5.97"	0.44"	68°	6.45"	0.43"	<0.04"
2	166°	4.01"	0.88"	158°	4.25"	1.10"	<0.08"
3	178°	4.37"	0.80"	170° - 215° *	4.84"	1.14"	<0.04"
4	184°	4.93"	0.84"	170° - 215° *	4.84"	1.14"	<0.04"
5	196°	4.77"	0.72"	170° - 215° *	4.84"	1.14"	<0.04"
6	210°	4.61"	0.44"	170° - 215° *	4.84"	1.14"	<0.04"
7	313°	5.89"	0.16"	Not Reported in 2001			
8	351°	4.77"	0.28"	345°	4.96"	0.43"	<0.04"
9	25°	5.85"	0.52"	18°	5.71"	1.02"	<0.04"

*Reported as multiple axial indications in 2002

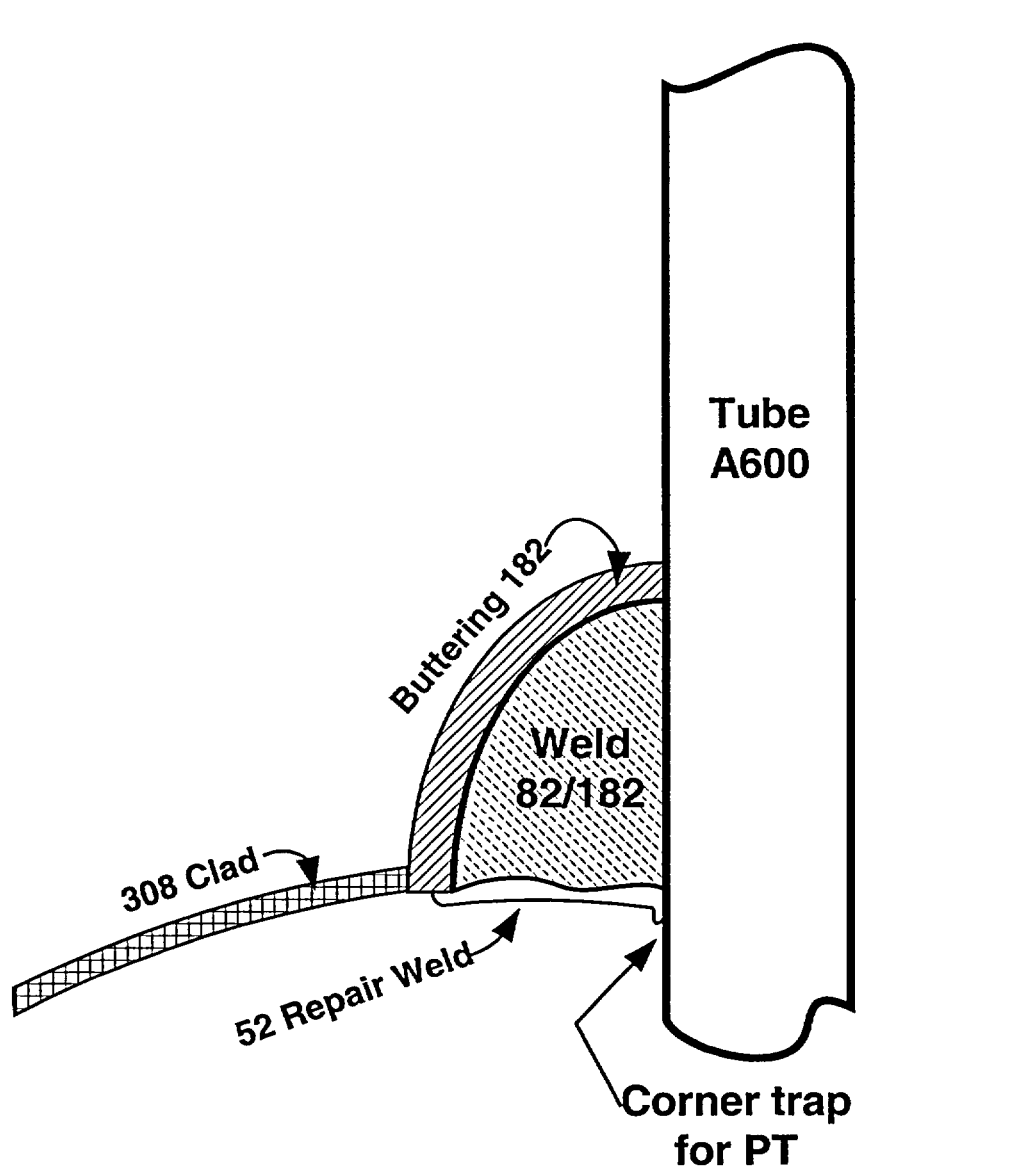


Figure 2-1 As-Repaired Configuration



Figure 2-2 Initial Liquid Penetrant Exam of Penetration 51, September 2002, First View

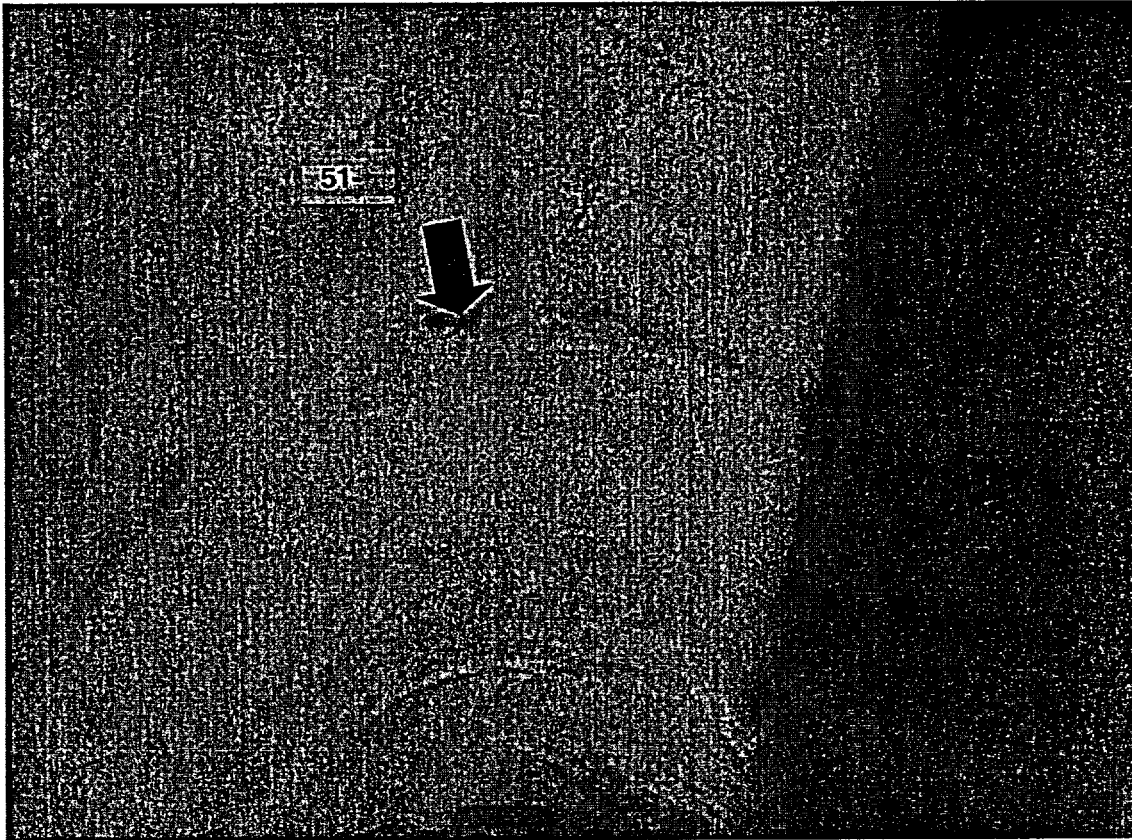


Figure 2-3 Initial Liquid Penetrant Exam of Penetration 51, September 2002, Second View

3 RESOLUTION OF INDICATIONS IN AND NEAR THE EMBEDDED FLAW REPAIR WELD

The indications on the inner periphery of the repair weld, near its boundary with the penetration tube, were the result of the geometry created by lack of blending of the weld layer to the tube surface. These indications were removed by blending to the tube interface, and verified by PT.

The remaining single indication was revealed after additional grinding was performed following the initial PT in September 2002.

All but one of the indications in the weld layer itself have been removed by grinding. With the initial grinding to a depth of 1/16th of an inch the indications were reduced in size by eighty percent or more, and in most cases eliminated. The final depth of the grinding to completely remove them has been estimated in Table 2-1.

The weld overlay repair is the same as any other corrosion resistant overlay. Its intended purpose is to provide a corrosion resistant barrier for the material underneath. The only examination requirement for a corrosion resistant overlay is a surface examination to provide reasonable assurance that no significant areas of the underlying material are still exposed to the environment. In most cases, as with the Code surface examination acceptance criteria, a few small, local, rounded indications are not a concern because not enough area of the underlying material is exposed to result in significant corrosion. In addition, multiple layers of overlay make it less likely that any indication would extend through the entire thickness of the overlay deposit. For the weld overlay being considered, the final surface layer did not exhibit any identifiable indications from the final dye penetrant examination.

Although the final post repair surface of the overlay was shown to be acceptable, there is no way of knowing what type of indications might lie just beneath the surface or what the size of those indications may be. Pickup of contaminants from the surface being welded on, entrapped gas, or other welding problems may create indications in the overlay material. As long as these indications are not surface breaking, they are generally not considered to be of any concern. These types of indications are most often found when the final overlay surface is disturbed which can result in a previous subsurface indication becoming a surface-breaking indication, as apparently occurred in the present case. This is not unique to this application and similar problems have occurred in other clad components when the surfaces were being reworked from the previously accepted surface. It is unfortunate that an as-found dye penetrant inspection of the overlay on this penetration was not performed prior to any material removal by flapper wheel or grinding operations. Such an examination, if performed, could have clearly demonstrated that the previously accepted surface was still intact.

Therefore, the weld overlay was acceptable for its intended purpose based on the results of the fall 2001 post repair dye penetrant examination performed on the final surface that was left exposed to the environment. The indications that were identified after the surface had been disturbed are not considered to impugn the integrity of the overlay.

The indications of most interest are those on the periphery of the weld, and these have been carefully studied, and some work is still underway. The most important finding here is that the repair weld did not

extend out far enough, and some of the Alloy 82/182 was left exposed to the PWR environment after the repair. This finding was verified on penetration 62, as described below.

In studying the penetrant results for penetration 62, it was noted that the repair weld was extended outward along the top portion to cover the area where the boat sample had been taken. The results of the boat sample were reported in reference [9] and showed that the boat sample was almost entirely in the buttering. Therefore, the extension of the weld repair in the upper portion of the penetration, in this case, fully covered the buttering. It seems possible that the indication at the bottom portion of this penetration may have resulted from the incomplete extension of the repair weld in that region.

To verify this theory, an acid etch was applied to the inside surface of the head, in the vicinity of penetration 62. The etchant solution was composed of the following proportions: 30 ml concentrated HCl, 20 ml H₂O, and 10 ml of 30% H₂O₂. The etching solution does not affect the Alloy 182 or Alloy 52 weld metal; but causes the stainless steel cladding to become dull, producing a contrast with the still - shiny Alloys 182 and 52. The results of the etch clearly showed an area of uncovered Alloy 182 in penetration 62 with a width of approximately 0.25 to 0.50 inches. This conclusion was possible because there is a clearly defined line at the edge of the Alloy 52 weld repair. A photo was taken of the etched region, and is shown in Figure 3-2.

A photo of penetration 62 showing the point at which the repair weld is extended outward to encompass the fall 2001 boat sample is shown in Figure 3-3. This photo shows the upper portion of the repair weld (approximately 120 degrees to 270 degrees) and no cracking is evident in this figure. A second photo taken in September 2002 (Figure 3-4) was taken to show the lower half of the penetration (approximately 340 degrees to 90 degrees), and in this case, penetrant, centered near the 350-degree location, and extending for approximately three inches, identified cracking. These cracks were concluded to be in the Alloy 82/182 weld.

Penetrations 51 and 63 were also etched, and the results did not conclusively demonstrate that the Alloy 182 weld metal was uncovered.

In addition to the region of Alloy 82/182, which was not completely covered, several indications around the periphery of the repair welds were found by PT. Two indications of this type in penetration 51 are being studied with a boat sample removed in September 2002.

These indications are shallow hot cracks in the Alloy 52 that originated during the welding process, and were revealed as surface indications as a result of grinding subsequent to the first PT. [More details on this finding will be provided when the boat sample analysis report is completed.]

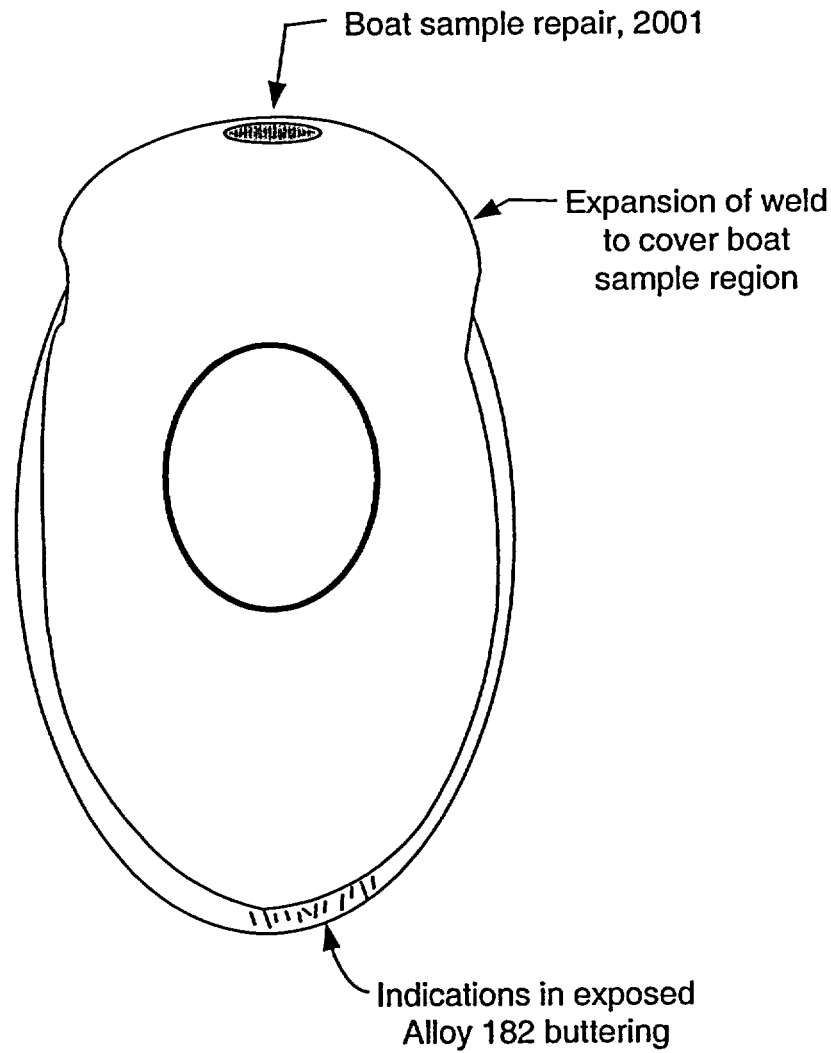


Figure 3-1 Sketch of Weld Repair on Penetration 62, showing the extension to cover the buttering and the portion of the butter that was exposed.



Figure 3-2 View of the Etched Region of the Penetration 62, September 2002
Showing the Region with the Lack of Weld Repair Coverage
The Boundary Between the Repair and the Original Weld Buttering is Shown
by the Solid Arrow. The Boundary Between the Buttering and the Etched
Stainless Steel (Gray) is Shown by the Small Red Arrows. The Area of PT
Indications is in the Buttering Between the Two Scribe Marks, Indicated by
the Large Open Arrows.



Figure 3-3 Penetrant Results of Penetration 62, September 2002, Showing the Extension of the Weld Repair Region to Cover the Boat Sample Region (See Arrow)

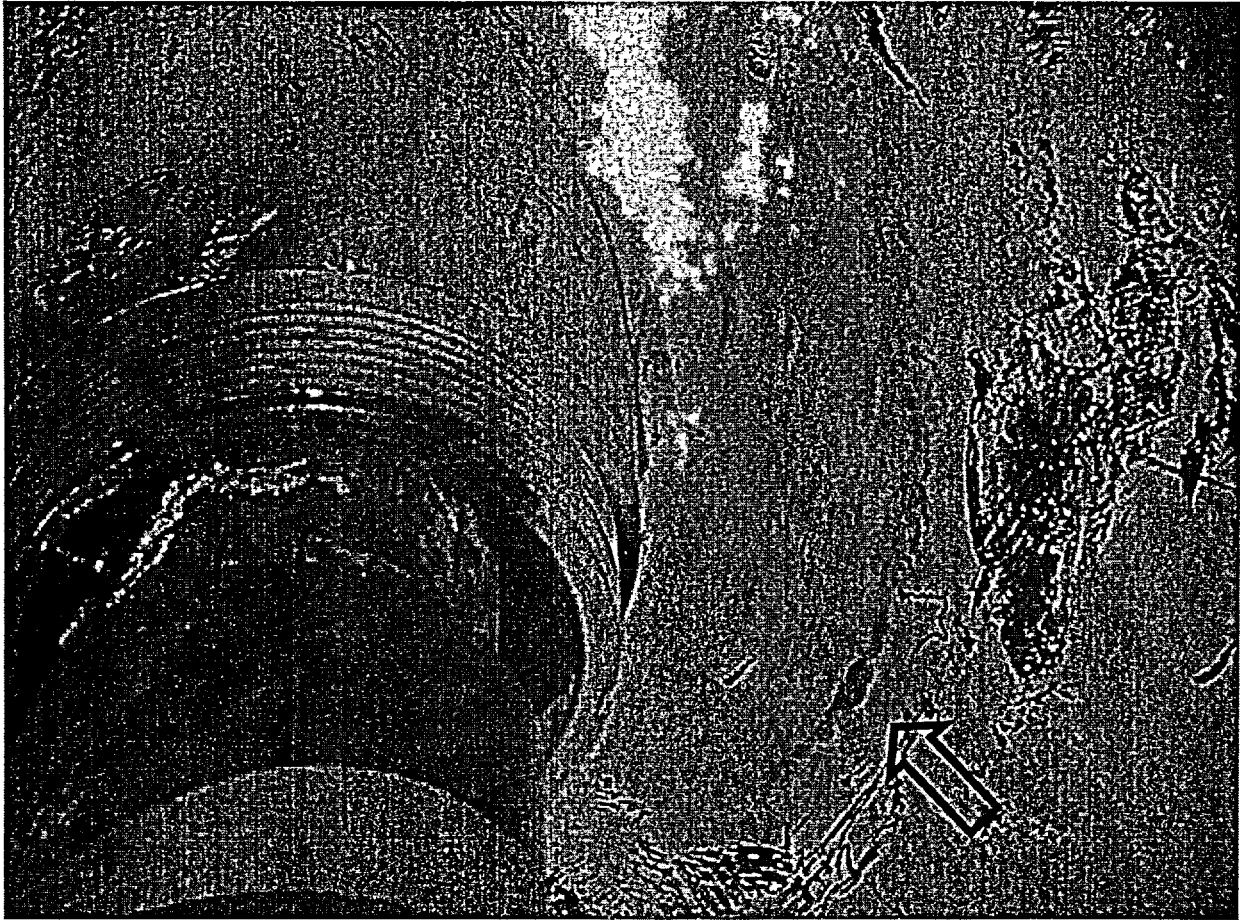


Figure 3-4 Penetrant Test Result for Penetration 62, Showing the Region of Cracking in the Original Weld, Where the Repair Weld did not Cover Completely (Cracking is Indicated by the Arrow)

4 BACKGROUND AND EXPERIENCE – SCC RESISTANCE OF ALLOY 52

4.1 INTRODUCTION

Alloy 52 is the filler metal used for the joining of Alloy 690 components by either the gas-tungsten arc welding (GTAW) or gas metal arc welding (GMAW) processes. The welding electrode used for the shielded metal arc welding (SMAW) process is Alloy 152. Both of these materials have compositions not differing greatly from the parent Alloy 690 material. Nominal compositions are provided in the following table.

Element	Alloy 690 Base Metal SB-167	Alloy 152 E-NiCrFe-7 SMAW	Alloy 52 ER-NiCrFe-7 GTAW/GMAW
C	0.05 max	0.05 max	0.04 max
Mn	0.5 max	5.00 max	1.00 max
Fe	7 to 11	7 to 12	7 to 11
P	-	0.03 max	0.02 max
S	0.015 max	0.015 max	0.015 max
Si	0.5 max	0.75 max	0.5 max
Cu	0.5 max	-	0.3 max
Ni	58 min	Bal	Bal
Co	-	-	-
Al	-	0.50 max combined	1.10 max Al or 1.50 max combined
Ti	-		
Cr	27 to 31	28.0 to 31.5	28.0 to 31.5
Nb + Ta	-	1 to 2.5	0.10 max
Mo	-	0.50 max	0.50 max
Other elements	-	0.50 max	0.50 max

Essentially coincident with the introduction of Alloy 690 as the material of choice for nuclear applications, Alloys 52 and 152 were introduced for fusion welding applications with 690.

The following paragraphs provide a summary of the experience with respect to these filler metals in service and in laboratory testing. As a point of interest, a summary of the background and corrosion resistance of Alloy 690 is provided in Appendix A. This summary was prepared to endorse the selection of Alloy 690 for SG tubing applications. It will be noted that, in view of the apparent immunity of Alloy 690 to PWSCC, nearly all of the testing reported in the literature cited has been in faulted secondary side chemical environments.

4.2 SERVICE EXPERIENCE

Steam Generators. The majority of the operating plant experience with Alloy 690 and the weld metals Alloys 52 and 152 is associated with replacement steam generator (SG) programs beginning in approximately 1994 with the Delta 75 replacements for V. C. Summer. In addition to the exclusive use of Alloy 690 for the SG heat transfer tubing applications, the weld metals were used for a range of applications in which contact with primary reactor coolant was required. A brief summary of the weld metal applications, primarily for Westinghouse-designed components, follows.

Plant	efpy	Component	Material	Application
New and Replacement Steam Generators				
V. C. Summer	7 +	SG nozzle welds	Alloy 52 and/or Alloy 152	Buttering over Alloy 82/Alloy 182 welds
		Safe end-nozzle welds		Final weld layer (in contact with RCS)
		Divider plate-channel head & stub runner		
N. Anna 1	7 +	Tubesheet cladding	Alloy 52 and/or Alloy 152	All buttering, cladding and welding operations
N. Anna 2	5 +	SG nozzle welds		
Kori 1	5 +	Safe end-nozzle welds		
Shearon Harris	3 +	Divider plate-tubesheet welds		
S. Texas 1	3			
S. Texas 2	1 +			
ANO-2	2			
Farley 1	2			
Farley 2	1 +			
Kewaunee	3			
Sequoyah 1	In mfg	Tubesheet cladding	A52/A152	
Ulchin 5 and 6	In mfg	Tubesheet cladding, nozzles, partial penetration welds	A52/A152	All buttering, cladding and welding operations
Other Components				
Sequoyah 1; N. Anna		Canopy seal overlays	A52/A152	
Mihama 1		CRDM replacements	A52/A152	Full penetration weld
Calvert Cliffs 1	2000	Quick-Lok repairs	A52/A152	Full penetration weld
Fort Calhoun, Waterford 3	1999, 2000	PZR nozzle repairs	A52/A152	Partial penetration welds
ANO 2; Palo Verde 2	2000	PZR heater sleeve repairs	A52/A152	Partial penetration welds
SONGS 2 & 3	1997-1998	PZR steam space and side shell nozzles; HL and CL A600 nozzle repairs	A52/A152	Partial penetration welds
D. C. Cook 2	~ 5 (1996)	CRDM nozzle repair	A52/A152	Overlay repair

In addition to these Westinghouse units, similar experience has been accrued with replacement SGs in Europe and in Japan, and in B&W replacement units for domestic PWRs.

There have been no reported instances of environmental degradation of any kind for any of these applications; this includes both the Alloy 690 base metal and the Alloy 52 or Alloy 152 weld metals.

This experience is fully consistent with expectations from laboratory testing performed to support the qualification of these materials. This class of austenitic nickel-base alloys, containing greater than 27 wt. pct. chromium, has exhibited full resistance to primary water stress corrosion cracking (PWSCC), to the extent that they are generally regarded as immune to this form of environmental degradation.

This experience, combined with the growing operating plant experience, also provided the basis for the use of Alloys 52 and 152 for the recent primary loop nozzle repairs at V. C. Summer.

Head Penetrations. The best example of service experience of an Alloy 52 weld repair is provided by the experience of the D. C. Cook Unit 2 embedded flaw repair. Penetration number 75 at this plant was found to have an inside surface flaw with a depth of approximately 40 percent of the tube wall thickness. This penetration was repaired with the embedded flaw repair process in 1996, and the repair was re-inspected in January of 2002.

The inspection of January 2002 was carried out with both dye penetrant and eddy current testing. The penetrant examination showed no indications, as did the eddy current testing. The eddy current results are more quantitative, and will be discussed here in some detail. The method was demonstrated and qualified under a program in response to the NRC Generic Letter 97-01. The process uses an eddy current coil with high-resolution gray scale imaging, with a magenta response at 50 percent of the amplitude of the calibration notch (0.004 inch long and 0.040 inch deep). This was shown empirically to correspond to the response to actual PWSCC. An example of such a response is shown in Figure 4-1, which shows actual clustered axial flaws in a penetration tube. The coil design is optimized for high spatial resolution, in order to distinguish individual responses among clusters of cracks, such as those shown in Figure 4-1.

This eddy current testing and display process was applied to the D.C. Cook penetration 75 in January 2002, and the results are shown in Figure 4-2. The results show no evidence of cracking after six years of service.

4.3 LABORATORY EXPERIENCE

For the reasons stated above, i.e., the fact that thorough laboratory testing and field experience to date have indicated no basis for concern over PWSCC with Alloy 690, relatively little testing for either crack initiation or crack propagation has been performed for either the base metal or the weld metals over the last ten or more years. The only research with which Westinghouse is familiar is cited below.

Psaila-Dombrowski et al. [10] evaluated the SCC resistance of Alloy 152 welds in primary water environments using constant extension rate tests (CERT) at 343°C (650°F). Examination of the fracture surfaces indicated no environmentally-related degradation. All fracture occurred by ductile rupture.

Psaila-Dombrowski et al. [11] performed a series of CERT tests on Alloys 52 and 152 weldments in simulated primary water at 343°C (650°F). After testing for periods up to 4122 hours, environmentally-related crack propagation was not observed.

These are the only published test results with which Westinghouse is familiar.

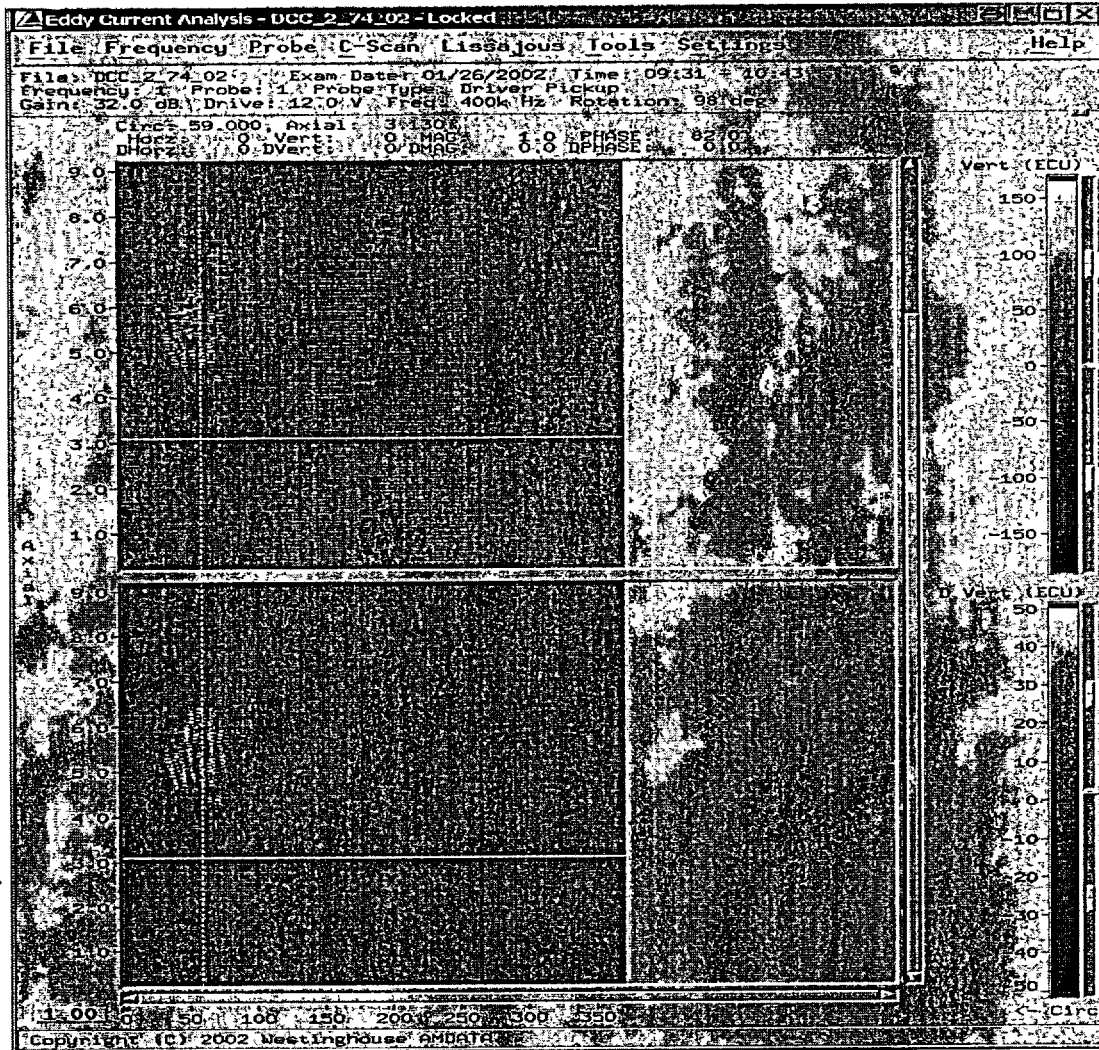


Figure 4-1 ECT View of Craze Cracking

5 REVISIONS TO THE EMBEDDED FLAW REPAIR PROCESS

Since the engineering evaluation concluded that the fundamental problem was inadequate coverage of the exposed Alloy 82/182 surface material, the obvious solution is to prevent this from occurring in the future. In the past, the edge of the Alloy 82/182 weld and butter were determined visually using the outer toe of the weld and surface grinding as indicators. What was presumed to be cladding may have, in fact, been the Alloy 82/182 weld metal. Design drawings were used as a guide, but as built dimensions of this region were not available.

There are two possible approaches to accomplish complete coverage of the Alloy 82/182 surfaces. One solution is to extend the weld overlay region outward for a sufficiently conservative extent so that the Alloy 182 butter would always be covered. This approach has the advantage of simplicity; however, the disadvantage is extra time and weld metal deposition. The extra weld metal would lead to additional penetrant testing coverage and the increased likelihood of in process repair grinding (and personnel exposure).

The alternative approach is to apply a nondestructive test to determine the boundary of the stainless steel clad to Alloy 182 surface. The technique of choice is an eddy current test that can distinguish the change in conductivity and permeability between stainless steel and Alloy 82/182. This method has been previously used during the inspection of an Alloy 82/182 safe end weld attached to a stainless steel clad reactor pressure vessel nozzle. Figure 5-1 shows actual field data employing this technique to identify the stainless/Alloy 82/182 boundary. In this image, a stainless steel pipe (upper green region) is attached to an Alloy 82/182 weld (middle blue region, which also has several crack indications) and then to the stainless steel clad vessel (lower green region). The demarcation between the Alloy 182/82 weld and the stainless cladding is very distinct.

In addition to this field data, additional qualification and procedure development has been conducted on a spare head located at the Westinghouse Waltz Mill facility as well as the North Anna 2 RPV head. In both cases, the boundary between Alloy 82/182 weld material and stainless clad is apparent in the data. Figure 5-2 shows a typical response from the North Anna 2 plant in which the stainless steel cladding is represented by the blue/green portion at the bottom of the eddy current test image.

The eddy current test probe will be mounted on the four axis manipulator tool delivery system so that a direct positional relationship can be established between the test coil and weld head. The nozzle region will be tested in approximately 45 degree increments to establish the cladding boundary. The welding process will cover this region plus 0.25 to 0.50 inches beyond this boundary. If the inspection results confirm that the construction drawings maximum tolerance dimensions can be used reliably to determine the boundary, then the additional inspection step may be deleted.

For acceptance inspection after the overlay, the weld surface will be subjected to the same penetrant test inspection as is currently conducted and the ASME code acceptance criteria of Section XI will be used. After one cycle of operation, a penetrant test will be conducted on the overlay weld surface. The weld surface will be cleaned with an approved solvent prior to inspection. Flapper wheel preparation will not be performed due to the possibility that innocuous inclusions or porosity may become exposed to the surface and produce irrelevant indications.

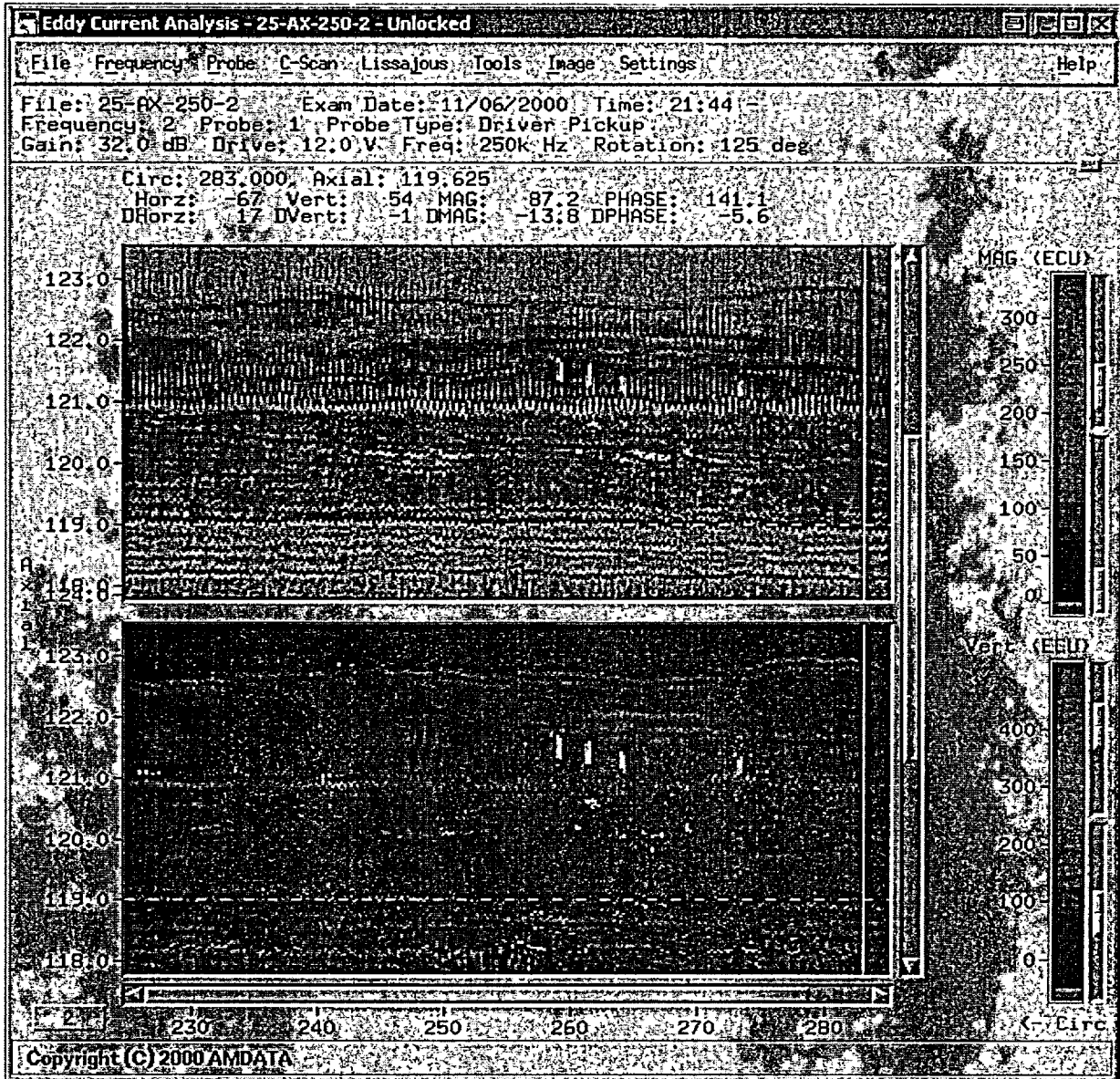
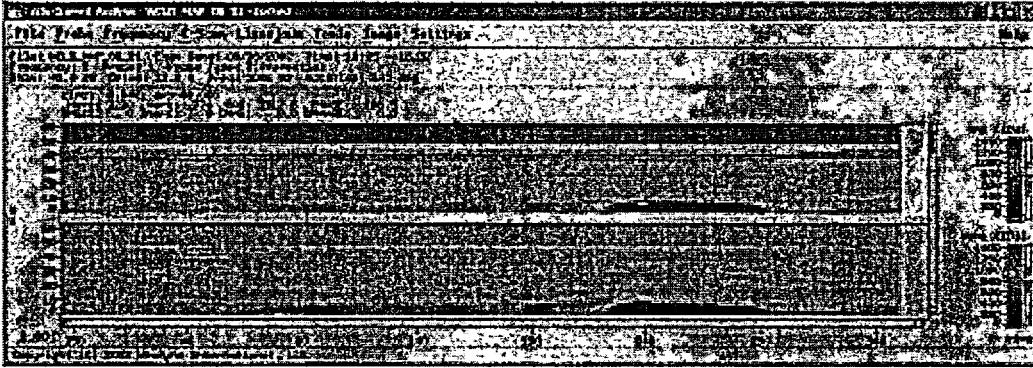
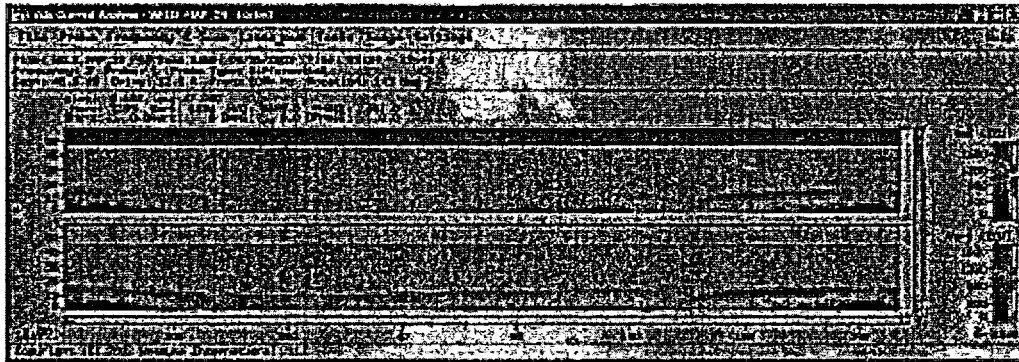


Figure 5-1 ET Result from Alloy 182 Safe End Weld Attached to a Stainless Steel Pipe (top) and Stainless Steel Cladding (bottom)



Weld Surface Mapping – C-Scan for CRDM No. 6



Weld Surface Mapping – C-Scan for CRDM No. 29

Figure 5-2 Eddy Current Test mapping of Alloy 182 weld to stainless steel cladding interface at North Anna 2

6 SUMMARY AND CONCLUSIONS

CRDM penetration tubes 51, 62 and 63 were repaired at the fall 2001 refueling outage by application of a weld overlay process with Alloy 52 weld metal. The weld overlay repair process is also referred to as the embedded flaw repair process. This application was the first site application of the weld overlay process on CRDM J weld surfaces. Post repair dye penetrant examination results were acceptable at all three J welds.

At the fall 2002 outage, dye penetrant indications were found at these same locations. As described in this report, these new indications have been evaluated and resolved in a number of different ways at specific locations. The indications at the penetration tube interface have been attributed to geometric discontinuities at that interface or to flapping. This evaluation has been demonstrated to be correct by light grinding to blend that local geometry and repeating the dye penetrant exams. The rounded indications in the surface of the repair welds are judged to be inclusions, not cracks, and have been removed by grinding; their removal was verified by re-examination.

The linear indications at the outer periphery of the weld overlay have been found, at least in penetration 62, to be PWSCC cracking in the original Alloy 182/82. The evaluations of these locations concluded that the weld repair did not provide an overlay on the entire exposed Alloy 182/82 surface, but instead stopped short of the stainless clad boundary. A few other indications exist along the outer periphery of the weld repair, and a boat sample was taken to further study these indications. Results of the boat sample confirm that the repair weld did not cover all of the exposed Alloy 82/182 material.

None of these issues challenge the basic technology that underlies the weld overlay, or embedded flaw repair. The Alloy 52 weld overlay material remains the appropriate material choice and the basic principle of providing a barrier between the reactor coolant and the original exposed Alloy 182/82 surfaces remains valid.

This evaluation does; however, demonstrate the need for process improvements and modifications for future applications of this repair. These corrective actions are described in Section 5 above, and consist of process modifications using proven, existing technology.

The application of this repair technique will be modified to reflect these evaluations and the indicated corrective actions.

7 REFERENCES

1. TR-109136, "Crack Growth and Microstructural Characterization of Alloy 600 PWR Vessel Head Penetration Materials," EPRI, December 1997.
2. WCAP-13998, "RV Closure Head Penetration Tube ID Weld Overlay Repair," March 1994. [Westinghouse Proprietary].
3. WCAP-15269, Rev. 1, "Aging Management Review and Time Limited Aging Analysis for the North Anna Units 1 and 2 Reactor Pressure Vessels," September 2001.
4. Rotterdam Welding Procedure 34.08, "Procedure for a combination of manual gas tungsten arc welding and manual gas metal arc welding of solid Inconel (P-Number 43) to solid Inconel (P-Number 43) or to Inconel weld overlay cladding."
5. Rotterdam Welding Procedure 37.02, "Procedure for manual shielded metal arc overlay cladding with Inconel (P-Number 43) of low alloy steel (P-Number 12B)."
6. Rotterdam Drawing 30660-1088, "Top Head Cap."
7. Rotterdam Drawing 30660-1097, "Top Head Cap (Pre Machined)"
8. Rotterdam Drawing 30660-1103, Sheet 1, "Closure Head Assembly C.R.D. Housing Assy."
9. Rao, G.V. and Bennetch, J., "Metallurgical Investigation of Cracking of the Alloy 82/182 J-Groove Weld of the Reactor Vessel Head Penetration Joint at North Anna Unit 2 Station," Westinghouse Report WCAP 15777, January 2002.
10. M. J. Psaila-Dombrowski et al., "Evaluation of Weld Metal 82 and Weld Metal 182 Stress Corrosion Cracking Susceptibility," *Proceedings, Seventh International Symposium on Environmental Degradation of Materials in Nuclear Power Systems – Water Reactors*, NACE Int'l., (1995) 81-91.
11. M. J. Psaila-Dombrowski et al., "Evaluation of Weld Metals 82, 152, 52 and Alloy 690 Stress Corrosion Cracking and Corrosion Fatigue Susceptibility," *Proceedings, Eighth International Symposium on Environmental Degradation of Materials in Nuclear Power Systems – Water Reactors*, ANS (1997) 412-421.

APPENDIX A

BASIS FOR SELECTION OF ALLOY 690 FOR STEAM GENERATOR HEAT TRANSFER TUBING

R. E. Gold and D. L. Harrod

A.1 INTRODUCTION AND SURVEY OF CORROSION RESISTANCE

The primary basis for the selection of a steam generator heat transfer tubing material is corrosion resistance. The corrosion behavior of Alloy 690TT in relevant steam generator environments, its performance relative to other prominent candidate tubing materials, namely Alloy 600, Alloy 800, and austenitic stainless steels, and a brief survey of recent corrosion research programs with this alloy, are reviewed in the following section. Following the summary and conclusions in the subsequent section, a selected list of references is given, and is complemented more completely in an attached Bibliography.

Corrosion Resistance of Alloy 690

Alloy 690 was adopted as the preferred alloy for steam generator heat transfer application in about 1986 after more than a decade of evaluation and testing. The first application of this alloy was in the replacement Series 54F steam generators at D.C. Cook Unit 2 in May 1989.

The basic corrosion resistance of thermally treated Alloy 690 (Alloy 690TT) to primary side or "normal" faulted secondary side environments had been fairly well established prior to its adoption. This research included the use of high temperature primary water and accelerated primary side environments such as 400°C doped steam to determine the primary side resistance, and testing in caustic, caustic-plus sulfate, caustic-plus CuO, and acid chloride environments for the secondary side. It was largely on the basis of the results of these tests that Alloy 690 was selected to replace mill annealed or thermally treated Alloy 600. At the present time, Alloy 690TT is the material of choice for all new and replacement steam generators built by Westinghouse, Framatome, Babcock & Wilcox International (BWI), and Mitsubishi Heavy Industries (MHI). Only Siemens is using an alternate material, Alloy 800 Mod.

Since the adoption of Alloy 690, laboratory-based research programs have continued on a modest basis. The primary intent of these efforts has been to determine whether or not a previously unidentified "Achilles Heel" exists for this material, or whether specific aspects of tube manufacturing might be modified to further optimize its corrosion resistance.

A brief survey of selected publications relevant to these efforts is provided in the following paragraphs. This survey is intended to be representative, rather than an exhaustive review of the available literature. A bibliography of Alloy 690 publications in the proceedings of International (refereed) Symposia in the period since approximately 1990 is appended to this report.

Recent Corrosion Testing of Alloy 690

In all corrosion tests used to simulate primary side environments Alloy 690TT continues to exhibit total immunity to primary water stress corrosion cracking (PWSCC). Hence, testing of this nature has essentially been abandoned.

Intergranular carbide precipitation has been demonstrated to enhance the stress corrosion cracking (SCC) resistance of nickel-chromium-iron alloys in nuclear steam generator environments. For Alloy 690TT, as was the case for Alloy 600TT, the intergranular carbide precipitation is achieved by a final thermal treatment at $\sim 720^{\circ}\text{C}$ for times from 5 to 15 hours. While the precipitation reaction occurs in fairly short times at this temperature, the extended time permits the replenishment of chromium to the region adjacent to the grain boundaries, thereby avoiding "sensitization."

That Alloy 690 contains 30% chromium, and therefore is much less susceptible to grain boundary chromium depletion than lower chromium compositions, offers the possibility that shorter-time higher-temperature thermal exposures may achieve the desired intergranular precipitation more efficiently than the $\sim 720^{\circ}\text{C}/5\text{-}15$ hour procedure. EPRI sponsored a research program in which caustic tests were performed on C-ring specimens of Alloy 690 tubing for which the thermal treatment was effected by 10-minute exposures at 871 or 927°C (Ref. 1). Alloy 690 specimens given standard thermal treatments were included for comparison. For the period of exposure, involving times up to 9000 hours, essentially no difference could be seen for tubing prepared using the various thermal treatments. However, in view of the perceived greater control afforded by the use of batch-loaded vacuum furnaces compared to continuous inert gas belt furnaces, none of the commercial tube manufacturers has continued with further evaluations of the higher-temperature, shorter-time thermal treatment process.

CIEMAT, the Spanish utilities' laboratory, has conducted tests comparing the stress corrosion cracking resistance of Alloy 600MA, Alloy 690TT, and Alloy 800 exposed at 350°C to the following environments (Refs. 2, 3):

Caustic Environments

- 10% NaOH
- 10% NaOH + 0.1M PbO (2% PbO)
- 10% NaOH + 0.01M PbO (0.2% PbO)
- 4% NaOH + 0.002M PbO (0.04% PbO)
- 10% NaOH + 0.01% CuO
- 50% NaOH + 5% $\text{Na}_2\text{S}_2\text{O}_3$ (sodium thiosulfate)

Acidic Environments

- 0.75M Na_2SO_4 + 0.25M FeSO_4
- 0.75M Na_2SO_4 + 0.25M FeSO_4 + 0.1M PbO (2% PbO)
- 0.4M NaHSO_4 + 0.2M FeSO_4 + 0.2M Na_2SO_4
- 50 ppm NaCl + 50 ppm CuCl_2

The 1000-hour exposures of the 2% strained C-rings showed clear superiority of Alloy 690TT over both Alloy 800 and Alloy 600MA in pure and CuO-doped NaOH. Alloy 690TT exhibited degradation only in

the 10% NaOH environments which contained PbO, and in the 50% NaOH + 5% sodium thiosulfate environment.

None of the acidic environments caused any degradation of Alloy 690TT, whereas they caused IGSCC of both Alloy 800 and Alloy 600MA. In all test environments, even those that caused some degradation, Alloy 690TT exhibited greater resistance to SCC than either Alloy 600MA or Alloy 800.

Vaillant et al. (Ref. 4) performed a series of 350°C corrosion tests to evaluate the relative role of mill annealing temperature, extent of grain boundary precipitation, and carbon content on the resistance of Alloy 690TT to SCC in NaOH solutions. NaOH concentrations of 4%, 10%, and 50% were used in pressurized capsule tests with applied stresses up to 90% of the 350°C yield strength. A range of Alloy 690 tubing products was tested, including materials that would not meet the current product specification with regard to grain size or grain boundary carbide density. After exposures up to 14,000 hours, the authors reported that Alloy 690 prepared with high final mill annealing temperature (> 1040°C and preferably > 1070°C), carbon content in the range 0.015 - 0.021%, and thermally treated to produce a high density of grain boundary carbides, exhibited optimum resistance to caustic SCC. The manufacturing specifications for Alloy 690TT meet these requirements.

Doherty et al. (Ref. 5) used 316°C constant extension rate tests (CERTs) in 10% NaOH to study the influence of minor microstructural differences on the corrosion resistance of Alloy 690TT. The test program was designed to include Alloy 690TT prepared by several different vendors and reflected variations in both the melting practice - e.g., air induction, argon-oxygen decarburization (AOD), vacuum-oxygen decarburization (VOD), or electroslag remelting (ESR) - and final tube reduction practice (pilgering or drawing).

The results of this test program were interpreted as confirming the importance of a high density of grain boundary carbides in enhancing the resistance to caustic SCC. No significant correlations could be drawn between the CERT results and tubing chemistry, level of intragranular carbides, inclusion content, melt practice, and mill anneal/thermal treatment practices. The authors suggest that the tube making process may be important but, conversely, state that the effect of tube making can not be demonstrated from their results since ... "The resultant microstructure for drawn tubing cannot be distinguished from that in pilgered tubing."

Sarver et al. (Ref. 6) also published the results of 316°C CERT tests in 10% NaOH of a variety of Alloy 690TT materials. Again, as in the previous discussion, the authors note the apparent importance of grain boundary carbide coverage in establishing caustic SCC resistance (but unfortunately do not provide microstructures to support this observation). They further conclude that no clear correlations were observed between chemistry or thermal processing and microstructure.

Sarver et al. (Ref. 7) have published additional research intended to identify the potential role of variations in manufacturing processes on microstructure and SCC resistance of Alloy 690TT. This research again used CERT tests in 10% NaOH at 316°C. The authors attempted to correlate small variations observed in the SCC resistance of Alloy 690TT produced by a variety of processes in terms of "grain boundary character distributions." They use, in this sense, the classification method devised originally by Watanabe (Ref. 8), whereby grain boundaries characterized by certain special or low angle crystallographic relationships (coincidence site lattice model) are expected to display special or improved

properties. Simply stated, the greater the density of these special, low energy, boundaries, the greater the resistance to SCC. The authors suggest that the relative ease with which these special boundaries apparently form in Alloy 690TT may have a significant role in its enhanced corrosion resistance. However, nothing presented, or referred to in the discussion which followed this presentation, identified how manufacturing processes may contribute to variations in this condition.

Several papers have been published recently documenting the results of corrosion tests of Alloy 690TT in caustic-plus-lead environments. This is, in fact, one of the few environments that can induce significant degradation in this alloy. McIlree (Ref. 9) and Sarver et al. (Ref. 10) reported the results of exposures of nine heats of Alloy 690 C-rings to a 4% NaOH-plus 125 ppm PbO environment at 324°C. The objective of these tests was to determine the influence of variations in the final mill annealing temperature and the thermal treatment time and temperature on the resistance to Pb-induced SCC.

Alloy 690 not given a thermal treatment cracked in times on the order of 1000 hours, with the lower temperature mill anneals being least resistant. The materials which exhibited the greatest resistance to SCC in 7000 hour exposures were those given relatively high temperature final mill anneals (> 1070°C). Little variation was seen over the range of thermal treatments. This latter observation is not particularly surprising since Pb-caustic SCC occurs in Alloy 690 by transgranular rather than intergranular cracking. The presence or lack of carbide precipitation at the grain boundaries would, therefore, be expected to play a relatively minor role.

The authors concluded that no clear correlations were observable between the resistance of Alloy 690 to Pb-caustic SCC and processing parameters (melting process, hot/cold working processes, final annealing temperature or thermal treatment practice). Neither were there any correlations between Pb-caustic SCC and material property parameters (chemistry, mechanical properties, grain size, inclusion rating, and carbide content and distribution). The Pb-caustic SCC appeared to be related solely to environmental test parameters, becoming more severe with increasing time, temperature, Pb concentration and stress. The Alloy 690TT tubing procured from Sandvik exhibited the best performance of all materials tested.

Included in the bibliography are a number of references which report the results of Pb-caustic SCC tests of Alloy 690TT. There is little question about the aggressiveness of this environment toward Alloy 690 - and Alloys 600 and 800 as well. The strategy that must be adopted by the utility is to take all possible measures to ensure minimal transport of lead into the secondary side SG water. Note that, with the exception of two instances - one in Canada and one in Europe - where Pb shielding blankets were inadvertently left inside SGs after maintenance operations, Pb-induced SCC has been a rarely observed form of degradation in SGs operating with Alloy 600 tubing.

Pierson et al. (Ref. 11, 12) have reported the results of a series of tests of Alloys 600, 690, and 800 in acidic environments at 320°C. The specimens were prepared as freestanding roll-expanded tube sections contained within capsules that contained the test environment. The cover gas was varied to include pure argon and argon containing 5% hydrogen. In the first phase of these experiments, acidic environments consisting of mixtures of Na₂SiO₃, Fe₃O₄ or FeSO₄, and cationic resins with and without dilute additions of PbO were found to very seriously degrade Alloy 600 and, to a lesser extent attack Alloy 800, in exposures ranging from 220 to greater than 2000 hours. For periods up to nearly 2000 hours, Alloy 690TT was fully immune to attack.

In a subsequent phase of this program, additions of approximately 0.1m concentrations of CuO and Cu₂O to these acidic environments induced significant cracking of Alloy 690TT when the cover gas was pure argon. When the cover gas contained 5% hydrogen, the Alloy 690TT did not crack. The testing was extended to determine if a dilute concentration of hydrazine (1 ppm), used to condition secondary water in many PWRs, would similarly inhibit degradation in the presence of copper oxides. Hydrazine was successful in this regard. The authors speculate that this inhibition effect may be due to a direct reduction of the copper oxides by the hydrogen or hydrazine. Several reviewers have acknowledged the results as reliable but have questioned the representativeness of the test conditions (artificial geometry, extremely high applied stresses, and a highly fictitious sludge composition). These reservations notwithstanding, these experiments enforce the position that during periods of wet layup and secondary side maintenance, it is prudent to maintain an active partial pressure of hydrogen or hydrazine, or as a minimum to ensure the exclusion of oxygen.

A.2 SUMMARY AND CONCLUSIONS – ALLOY 690TT CORROSION RESISTANCE

Alloy 690TT was chosen for SG heat transfer tubing applications on the basis of its superior corrosion resistance. This was true in the mid-1980s and remains true today. None of the recent corrosion test results suggest any basis for changing or revisiting this decision. In virtually every head-to-head comparison of Alloy 690TT with Alloy 800 Mod, Alloy 690TT continues to demonstrate superior performance.

Several years ago, Westinghouse collaborated with the Electric Power Research Institute in developing a summary comparison of the relative corrosion resistance of Alloy 600MA, Alloy 600TT, Alloy 690TT, Alloy 800 Mod, and austenitic stainless steels in a broad range of corrosive environments. This summary is presented in Table 1. Only in the area of Pb-caustic corrosion does Alloy 690TT fare poorly, as discussed above; this is true, however, of the other alloys as well, although Alloy 600 performs slightly better than the other candidates.

Although this ranking was developed five or six years ago, a close review indicates that no data of which Westinghouse is aware would alter the rankings indicated. The ranking of Alloy 690TT is particularly impressive when the excellent field performance of Alloy 800 Mod is acknowledged. This latter alloy, which clearly offers lower resistance to attack in both acid chloride and caustic environments than Alloy 690TT, has established an impressive performance history in German PWRs over the last twenty or so years. It seems reasonable to expect Alloy 690TT to perform even better.

A.3 SUMMARY AND CONCLUSIONS

Alloy 690 was selected as the heat transfer tubing material for replacement steam generators. The primary basis for this selection is the demonstrated superior corrosion resistance of Alloy 690TT to other candidate tubing materials (Alloy 600 and Alloy 800) in all relevant primary side and secondary side steam generator environments. A brief update on the status of recent additions to the corrosion data base for Alloy 690TT was also presented herein. Alloy 690TT fully satisfies all other specification requirements for SG heat transfer tubing. Since the initial selection of Alloy 690 in the mid-1980s, all additional data and information acquired to date further endorses that selection.

A.4 REFERENCES

1. EPRI NP-6703-M, "Effect of Different Thermal Treatments on the Corrosion Resistance of Alloy 690 Tubing," Final Report on Project S408-2, March 1990.
2. CIEMAT (Spain), Untitled presentation on the Comparative Performance of Alloys 600, 690 and 800 in Caustic, and Caustic-plus-other Contaminant Environments, EPRI IGA/SCC Workshop, Airlie, VA, May 1991.
3. M. L. Castano-Marin et al., "Steam Generator Replacement: Inconel 690 TT and Incoloy 800 Mod. as an Alternative to Inconel 600," presented at the European Corrosion Conference Meeting, Barcelona, Spain, July 1993.
4. F. Vaillant et al., "IGSCC Resistance of Alloy 690 in Caustic Solutions," presented at EPRI Steam Generator IGA/SCC Workshop, Minneapolis, MN, October 14-15, 1993.
5. P. E. Doherty et al., "Stress Corrosion Cracking (SCC) Behavior vs. Microstructure for Alloy 690 Steam Generator Tubing," Second International Steam Generator & Heat Exchanger Conference, Toronto, Canada, June 13-15, 1994.
6. J. M. Sarver et al., "Constant Extension Rate (CERT) Testing of Alloy 690 and Alloy 800 Nuclear Steam Generator Tubing," International Symposium - Fontevraud III, Fontevraud, France, September 12-16, 1994, pp. 529-536.
7. J. M. Sarver et al., "The Influence of Manufacturing Processes on the Microstructure, Grain Boundary Characteristics and SCC Behavior of Alloy 690 Steam Generator Tubing," Proc. Seventh International Symposium on Environmental Degradation of Materials in Nuclear Power Systems - Water Reactors, Breckenridge, CO, Aug. 7-10, 1995. Published by NACE; pp. 465-476.
8. T. Watanabe, *J. Physics*, **46**, C4-555 (1985).
9. A. R. McIlree, "Influence of Heat Treatment on the SCC Behavior of Alloy 690 in a Pb-Contaminated Solution," presented at EPRI Technical Advisory Group Meeting, Charlotte, NC, February 7-9, 1996.
10. J. M. Sarver et al., "A Parametric Study of the Lead-Induced SCC of Alloy 690," Proc. Eighth International Symposium on Environmental Degradation of Materials in Nuclear Power Systems - Water Reactors, Amelia Island, FL, Aug. 10-14, 1997. Published by ANS; pp. 208-215.
11. E. Pierson et al., "Resistance en milieu acide des materiaux alternatifs pour tubes de GV (Alliages 690 et 800)," International Symposium - Fontevraud III, Fontevraud, France, September 12-16, 1994, pp. 556-564.

12. E. Pierson et al., "Stress Corrosion Cracking of Alloys 690, 800 and 600 in Acid Environments Containing Copper Oxides," presented at CORROSION 96, paper 96119, NACE International.
13. EPRI NP-6996-SD, "Alloy 690 for Steam Generator Tubing Applications," Final Report on Project S408-6, October 1990.

A.5 BIBLIOGRAPHY ALLOY 690 LITERATURE - INTERNATIONAL FORUMS (SINCE CA. 1990)

Fontevraud INTERNATIONAL SYMPOSIA

Fontevraud I – 2–6 September 1985 (First in Series)

- C. Gimond et al., "Choix de l'alliage 690 pour les tubes de Generateur de Vapeur," pp. 270–279.
- T. Yonezawa et al., "Effect of Heat Treatment on Corrosion Resistance of Alloy 690," pp. 289–296.

Fontevraud II – 10–14 September 1990 (Second in Series)

- G. P. Airey et al., "Inconel 690 Steam Generator Tubing: Material Specification and Corrosion Resistance," pp. 408–417.

Fontevraud III – 12–16 September 1994 (Third in Series)

- N. Hakiki et al., "Etude des films d'oxyde formes sue les alliages a base de nickel 600 et 690 et l'acier inoxydable 316L en milieu primaire," pp. 327–336.
- M. A. Kreider et al., "Corrosion Mode Diagrams for Alloy 690 TT and Alloy 800," pp. 521–528.
- J. M. Sarver et al., "Constant Extension Rate (CERT) Testing of Alloys 690 and 800 Nuclear Steam Generator Tubing," pp. 529–536.
- A. Rocher et al., "Effect of Lead on the OD Degradation of Steam Generator Tubes," pp. 537–547.
- E. Pierson et al., "Resistance in milieu acide des materiaux alternatifs pour tubes de GV (Alliages 690 et 800)," pp. 556–564.
- M. Garcia et al., "Effect of Lead on Inconel 690 and Incoloy 800 Oxide Layers," pp. 571–578.

Fontevraud IV – 14–18 September 1998 (Fourth in Series)

- R. Staehle and Z. Fang, "SCC of Inconel 600 and Inconel 690 in the Mid-Range of pH," pp. 369–380.
- P. E. Doherty, et al., "The Corrosion Performance of Alloy 690 Steam Generator Tubing - An Overview," an attachment to published proceedings.
- T. Larsson and J.-O. Nilsson, "The Influence of Manufacturing Process on Texture and Grain Boundary Distribution in Alloy 690," pp. 595–604.
- P. R. Aaltonen, et al., "The Effect of Environment on the Electric and Electrochemical Properties of Surface Films on Alloy 600 and Alloy 690 in Pressurised Water Reactor Primary Water," pp. 861–872.

INTERNATIONAL SYMPOSIA ON ENVIRONMENTAL DEGRADATION OF MATERIALS IN NUCLEAR POWER SYSTEMS - WATER REACTORS**Fourth International Symposium. Published by NACE. August 6-10, 1989; Jekyll Island, FL.**

- D. B. Lowenstein et al., "Etching Techniques and Carbon Analysis for Alloy 690," pp. 5-1 – 5-15.
- J. R. Crum et al., "Contribution to Optimized Specifications for Procurement of Inconel Alloy 690 PWR Steam Generator Tubing," pp. 5-16 - 5-32.
- A. Smith and R. Stratton, "Relationship Between Composition, Microstructure and Corrosion Behaviour of Alloy 690 Steam Generator Tubing for PWR Systems," pp. 5-33 – 5-46.
- J. M. Sarver et al., "The Effect of Thermal Treatment on the Microstructure and SCC Behavior of Alloy 690," pp. 5-47 – 5-63.
- T. M. Angeliu and G. S. Was, "Grain Boundary Chemistry and Precipitation in Controlled Purity Alloy 690," pp. 5-64 – 5-78.
- P. Combrade et al., "Effect of Sulfur on the Protective Layers on Alloys 600 and 690," pp. 5-79 – 5-95.
- K. Yamanaka et al., "Straining Electrode Behavior and Corrosion Film of Nickel Base Alloys in High Temperature Caustic Solution," pp. 5-96 – 5-106.
- J. M. Sarver et al., "Qualification of Kinetically Welded Alloy 690 Sleeves," pp. 5-107 – 5-127.

Fifth International Symposium. Published by ANS. August 25–29, 1991; Monterey, CA.

- K. Norring et al., "Grain Boundary Microstructure, Chemistry, and IGSCC in Alloy 600 and Alloy 690," pp. 482–487.
- D. L. Harrod et al., "The Temperature Dependence of the Tensile Properties of Thermally Treated Alloy 690 Tubing," pp. 849–854.
- A. J. Smith and R. P. Stratton, "Thermal Treatment, Grain Boundary Composition and Intergranular Attack Resistance of Alloy 690," pp. 855–859.
- S. Suzuki et al., "IGA Resistance of TT Alloy 690 and Concentration Behavior of Broached Egg Crate Tube Support Configuration," pp. 861–868.
- Sixth International Symposium. Published by TMS. August 1-5, 1993; San Diego, CA.
- A. J. Smith et al., "The Effect of the Weld Thermal Cycle on the Microstructure and Corrosion Resistance of Alloys 690, 600 and 800," pp. 97–104.
- S. B. Justus and J. J. Eckenrod, "P/M Alloy N690 as a Solution for Intergranular Stress Corrosion Cracking," pp. 113–120.
- M. Helie, "Lead Assisted Stress Corrosion Cracking of Alloys 600, 690 and 800," pp. 179–188.
- W. H. Cullen et al., "Corrosion of Alloys 600 & 690 in Acidified Sulfate and Chloride Solution," pp. 197–206.

Seventh International Symposium. Published by NACE. August 7–10, 1995; Breckenridge, CO.

- D. Costa et al., "Interaction of Lead with Nickel-Base Alloys 600 and 690," pp. 199–208.
- F. Vaillant et al., "Comparative Behavior of Alloys 600, 690 and 800 in Caustic Environments," pp. 219–232.
- K. K. Chung et al., "Lead Induced Stress Corrosion Cracking of Alloy 690 in High Temperature Water," pp. 233–246.
- J. M. Sarver et al., "The Influence of Manufacturing Processes on the Microstructure, Grain Boundary Characteristics and SCC Behavior of Alloy 690 Steam Generator Tubing," pp. 465–476.
- D. A. Mertz et al., "Role of Microstructure in Caustic Stress Corrosion Cracking of Alloy 690," pp. 477–494.
- K. Liu et al., "Effect of Sulfur and Magnesium on Hot Ductility and Pitting Corrosion for Inconel 690 Alloy," pp. 509–518.

Eighth International Symposium. Published by ANS. August 10–14, 1997; Amelia Island, FL.

- J. R. Crum and T. Nagashima, “Review of Alloy 690 Steam Generator Studies,” pp. 127–137.
- J. Frodigh, “Some Factors Affecting the Appearance of the Microstructure in Alloy 690,” pp. 138–148.
- H. Kajimura et al., “Corrosion Resistance of TT Alloy 690 Manufactured by Various Melting Practices in High Temperature NaOH Solution,” pp. 149–156.
- P. E. Doherty et al., “Mechanical-Electrochemical Performance of Alloy 690 Steam Generator Tubing,” pp. 157–166.
- S. S. Hwang et al., “Stress Corrosion Cracking Aspects of Nuclear Steam Generator Tubing Materials in the Water Containing Lead at High Temperature,” pp. 200–207.
- J. M. Sarver et al., “A Parametric Study of the Lead-Induced SCC of Alloy 690,” pp. 208–215.
- H. Takamatsu et al., “Study on Lead-Induced Stress Corrosion Cracking of Steam Generator Tubing Under AVT Water Chemistry Conditions,” pp. 216–223.
- G. Sui et al., “Stress Corrosion Cracking of Alloy 600 and Alloy 690 in Hydrogen/Steam and Primary Side Water,” pp. 274–281.
- M. J. Psaila-Dombrowski et al., “Evaluation of Weld Metals 82, 152, 52 and Alloy 690 Stress Corrosion Cracking and Corrosion Fatigue Susceptibility,” pp. 412–421.
- I. Bobin-Vastra, “Preoxidation of SG Alloy 690 Tubes to Decrease Metal Loss in the Primary Circuit: A Laboratory Study,” pp. 507–513

APPENDIX B

METALLURGICAL EVALUATION OF AN EMBEDDED FLAW REPAIR SAMPLE REMOVED FROM THE NORTH ANNA UNIT 2 RPV HEAD

W. R. Gahwiller

B.1 INTRODUCTION

In order to evaluate the condition and extent of the Embedded Flaw Repair performed on the North Anna No. 2 RV Head, a metallurgical "boat" sample was removed from the Nozzle No. 51 repair made during the fall 2001 outage. The decision to remove the particular sample was based on data described in the main body of this report. The sample was shipped to the Westinghouse Science and Technology Department hot cell in Pittsburgh for metallurgical examination. This report describes these examinations and provides an assessment of the repair as represented by this sample.

B.2 OBJECTIVES AND METHODOLOGY

The initial objectives of this evaluation were to (1) characterize the nature of the dye penetrant (PT) indications described in Section 2 and Table 2-1, (2) characterize the extent and nature of the weld repair, and (3) determine whether any evidence of a leak path existed that would explain the leakage found on the RPV Head at the Nozzle No. 51 location

The methods used to perform this evaluation consisted of optical and scanning electron microscopy (SEM) as well as Energy Dispersive Spectrographic (EDS) semi-quantitative chemical analysis of selected surfaces.

B.3 SAMPLE EXAMINATION

As-Received Description

The boat sample was removed, using the electrodischarge machining (EDM) process, in such a manner as to locate the PT indications at 135° approximately in the center of the sample. Figure B-1 is a sketch of the radial location of the sample relative to the J-Weld, J-Weld Butter, and Stainless Steel cladding. The as-received sample consisted of a piece approximately 2.75 inches long, 0.5 inch wide (Figure B-2A) and 5/8 inch deep (Figure B-2B). The sample was oriented such that the long axis was tangential to the circular weld repair.

Visual examination of the sample revealed three distinct areas on the wetted surface. The first consisted of a relatively flat, more oxidized surface along the outer most edge, the second a partial arc of three weld beads running approximately longitudinally along the sample, and third a depressed area intersecting the flat surface and the outer two weld beads. These areas are depicted in Figures B-2A and B-3.

Wetted Surface Examination

The complete surface depicted in Figure B-2A was examined by optical and scanning electron microscopy at up to 40X. The three weld beads exhibited the characteristic solidification pattern with some areas indicating that a slight amount of metal had been removed from the top of the ridges. No cracks were evident on the weld beads or flat surfaces. Examination of the depression, however, revealed this area contained cracks open to the surface in the location of the PT indications. Further, this region exhibited grooving indicative of a ground surface. Figure B-4 is a macrophotograph of the cracks and the surrounding surface.

Weld Bead Evaluation

In order to characterize the weld repair, a number of evaluations were performed both on the as-received surface and on metallographic cross sections taken as shown in the layout in Figure B-3. In general, evaluation consisted of examining the sections for evidence of defects as well as performing EDS semiquantitative chemical analysis of various areas to differentiate the weld repair from the original fabrication weld and provide data with respect to the cause of any observed defects.

As-Received Surface

EDS analysis was performed on the as-received surface both in the ground area containing the surface cracks and on the original weld bead wetted surfaces. The locations of these analyses are shown in Figures B-2A and B-4 and the results contained in Table B-1. The interpretation of these results is as represented in Figure B-5.

Transverse Sections

Sections A-A and C-C (Figure B-3) were taken transverse to the boat sample long axis at a location away from the surface cracks. Section A-A was located such that it intersected the ground region while C-C was taken through a portion exhibiting the original weld bead profile. The sections were polished and etched to show the weld bead configuration. EDS analysis was performed at various locations representative of the different weld beads observed. Figures B-6A and B-6B show the weld structure as well as the location and results of these analyses.

Longitudinal Sections

Sections B1, B2, and B3, shown in Figure B-4, were cut approximately parallel to the long axis of the sample. Section B1 (Figure B-7) was cut, mounted, and ground such that examination was performed in the outboard direction at the tip of the larger surface crack shown in Figure B-2. Section B2 (Figure B-8) was taken looking inboard on the opposing cut surface. Due to the blade thickness, this surface is approximately 1/16 inch away from surface B1 (Figure B-3). Section B3 was prepared by breaking the piece with B2 out of the metallurgical mount and grinding the inboard surface of the sample until the stainless steel cladding was exposed for the complete length of the sample. The view shown in Figure B-9 is looking outboard at this surface.

Repair Weld Characterization

In order to differentiate weld beads as a result of the original fabrication or the embedded flaw repair, the nickel, iron, chromium, aluminum, titanium, and niobium content of the weld metal was investigated. In some cases such as when the chromium content of the weld metal was near the 28.1% reported in the CMTR for the Alloy 52 (ERNiCrFe-7) utilized, or the composition of the underlying metal is close to that of the weld metal, this assessment is performed by inspection. In other cases, particularly where considerable dilution had occurred, an expected composition was calculated for each of the potential filler metals. This was accomplished by calculating a percent dilution based on the nickel and iron contents then applying that factor to the other elements in the filler metal. A comparison was then made with the measured composition and a determination made as to the most likely filler metal. Percent dilution was calculated by:

$$\%D = 100[(E_{WM} - E_{FM}) / (E_{BM} - E_{FM})]$$

where:

- E_{WM} = The element weight percent in the deposited Weld Metal
- E_{FM} = The element weight percent in the undiluted Filler Metal
- E_{BM} = The element weight percent in the Base Metal being welded on. In multi-pass welds this is represented by the composition of the previous weld pass.

Section A-A and C-C

With the exception of differences in the depth of the original Alloy 52 J-Weld cover pass, the results of Sections A-A and C-C are very similar. Comparison of the filler metal evaluations shown in Figures B-6A and B-6B with those of the as-received surface shows that there is considerable agreement with the determinations from Figure B-2 as to the A-52 composition of the Inboard and Middle beads. Although consistent with a starting filler of A-82/182, the Outboard bead shown in Section A-A exhibits a higher degree of dilution than that of the surface examination or Section C-C. This can be explained by the greater penetration for that bead shown in Section A-A as compared with Section C-C.

Section B1

Section B1 shown in Figure B-7 contains the tip of the PT indication as well as several other fissures near the ground surface. A continuous 0.075 inch thick weld bead layer exists on top of the austenitic stainless steel clad surface, on which there exists an intermittent weld bead. This configuration is created by the intersection of the plane of B1 with the very outboard edge of a second weld pass.

The EDS analysis identifies the continuous weld bead as highly diluted Alloy 82 with the intermittent weld pass representative of moderately diluted Alloy 52. The fissuring is associated exclusively with the interface between the continuous and the intermittent weld beads in this cross section. No fissures were observed in any other area of the original Alloy 82 fabrication weld. This is consistent with reheat

cracking occurring in the Alloy 82 and propagating into the thin layer of Alloy 52 at the edge of the repair weld bead.

Section B2

Section B2 (Figure B-8) is characterized by three continuous weld beads on top of the stainless steel clad. As with Section B1, the analysis shown in Figure B-8A indicates the first layer is highly diluted Alloy 82/182 and the second most likely moderately diluted Alloy 52. The third layer is characteristic of a lightly diluted Alloy 52 with an average thickness of 0.040 inch. Whereas the nominal thickness of each repair bead is approximately 1/16 inch, this layer represents only 2/3 of a repair pass. While this section contains more fissures and hot cracks than B1, once again they are associated with the interface between the diluted beads with none of the fissures intersecting the ground surface of the partial Alloy 52 repair.

Section B3

Section B3, (Figure B-9), located less than 1/4 inch from Section B2, contains only two fissures located at the interface between a thin apparent Alloy 82 first layer and the first layer of the Alloy 52 repair. At this radial location in the repair, the Alloy 52 penetrates to the stainless steel clad over most of the sample length. No fissures are present over this Alloy 52 / 308 clad interface. The chemical composition of the Alloy 52 is such that the nickel content is at or above 49% whereas in the Alloy 82 portion it is about 43%, similar to other areas that have experienced hot cracking. Given that the Alloy 52 exhibits a full thickness repair of 0.150 inch with little dilution (less than 25% for the first layer and less than 10% for the second) indicates that the basic repair procedure can be applied with little possibility of reheat or hot cracking near the wetted surface.

One additional anomaly was observed at the surface (Figure B-9 Area B) of this section. As shown by the SEM view and EDS spectra in Figure B-9B, a tungsten inclusion was present on the edge of the sample. It is likely that such an inclusion could have resulted in the rounded PT indication reported at the 125° location, either originally as a small non-relevant indication or later after abrasive flapper wheel cleaning partially removed it producing a more noticeable indication.

B.4 DISCUSSION

In summary, the wetted surface outermost bead is consistent with Alloy 82 as demonstrated by its lower chromium content, a reasonable level of niobium, and lower levels of aluminum and titanium. Conversely, the inner two wetted surface weld beads are consistent with Alloy 52 with its higher chromium content, lack of niobium, and higher aluminum plus titanium. Subsurface weld beads were more difficult to identify in that compositions combined with the tolerance on the EDS analyses could result from either Alloy 82/182 or Alloy 52.

As can be seen from the metallurgical sections, various frequencies of fissures exist in the underlying weld metal. They occur at the interface between weld beads where the underlying weld metal is susceptible to reheat cracking as a result of excessive dilution. The reheat cracks propagate into the liquid weld metal forming hot cracks, which are also more prevalent when considerable dilution has occurred. The morphology of these fissures is consistent with the hot cracks identified in the original North Anna Unit 2 J-Weld buttering investigation reported in Reference 6.1 and with hot cracks and/or ductility dip

cracking identified by others (References 6.2 and 6.3). Although they exhibit varying widths in the circumferential direction due primarily to shrinkage stresses in that direction, they tend to be short in both the thickness and radial direction.

Unlike the cracking in the previous North Anna sample examination, there are no tight, singular cracks consistent with PWSCC or other environmentally associated degradation.

As can be seen from the location of hot cracks and the approximate chemical analyses shown in Table B-1 and Figures B-6 through B-9, cracking was found in layers where the weld filler metal dilution exceeded 30%. This generally resulted in a nickel content of less than 50% and an iron content exceeding 30%. Reference 6.3 mentions the potential for hot cracking in Alloy 52 and 82 when dilution levels are higher than 25-30%. This is consistent with results reported in References 6.4 where it has been reported that Ni-Cr Fe- alloys with nickel content below 50% are prone to hot cracking.

The observations described above with respect to the limited radial extent of the Alloy 52 repair and the crack morphology may explain why easily removed linear PT indications could have been present at the toe of the repair weld both in the as-welded and/or mechanically worked condition. Shallow reheat cracks might be expected to form on the surface or slightly subsurface in the highly diluted Alloy 82 deposit. This would also be consistent with the fact that small linear indications may have been present after the relatively small amount of metal removed by the flapper wheel treatment of the repair weld during the 2002 outage.

By contrast, the chemical composition of the two layers of Alloy 52 shown in Figure B-9A representing a full thickness repair of 0.151 inch indicates that the gas tungsten arc machine weld repair procedure produced only a limited amount of dilution. Therefore, the application of Alloy 52 onto the 308 type cladding did not result in hot cracking because there was insufficient dilution of the filler metal to make the Alloy 52 susceptible. Additionally, except for the small area at the clad interface in Area A, there was no reheat cracking susceptible layer of highly diluted Alloy 82/182.

The final assessment is that the cracks that were found were short and reasonably isolated. This, in addition to the fact that no leak path exists from the repair weld, past the cladding, to the J-Weld, indicates that these cracks are not the source of any O.D. RPVH leakage.

B.5 CONCLUSIONS

- Contrary to the repair weld intent, the original construction Alloy 82 was not completely covered with Alloy 52 weld metal.
- Examination of the boat sample surface indicated no cracks or fissures in the as-repaired wetted surface.
- The linear dye penetrant indications were a result of sub-surface hot cracking exposed to the surface by inadvertent grinding of the weld bead during the fall 2002 outage.
- The rounded dye penetrant indication was most probably due to a tungsten inclusion at the weld surface.

- The two layer repair weld procedure, when extended to the austenitic stainless steel cladding beyond any original Alloy 82/182 deposit, is capable of producing an acceptable final weld surface.
- None of the cracking, observed on the boat sample, was of a configuration that could define a leak path.
- None of the indications or subsurface cracking was environmentally associated.

B.6 REFERENCES

1. Rao, G.V., et al, Metallurgical Investigation of Cracking of the Alloy 82/182 J-Groove Weld of the Reactor Vessel Head Penetration Joint at North Anna Unit 2 Station, WCAP-15777, January 2002.
2. Kiser, S. D., Discussion of Hot and Ductility Dip Cracking in Inconel 52 /152 Weld Metal, Special Metals Welding Products Company, December 2000.
3. Lin, W. and Lippold, J., Weldability Testing of Inconel Filler Materials, Edison Welding Institute Final Report J5990 to Westinghouse Electric Corp, December 1992, presented at EPRI-IAII Nuclear Welding Symposium, October 1993, Charlotte, NC
4. Communication on Japanese Patent No. 10-314937, Babcock Hitachi KK, 1998

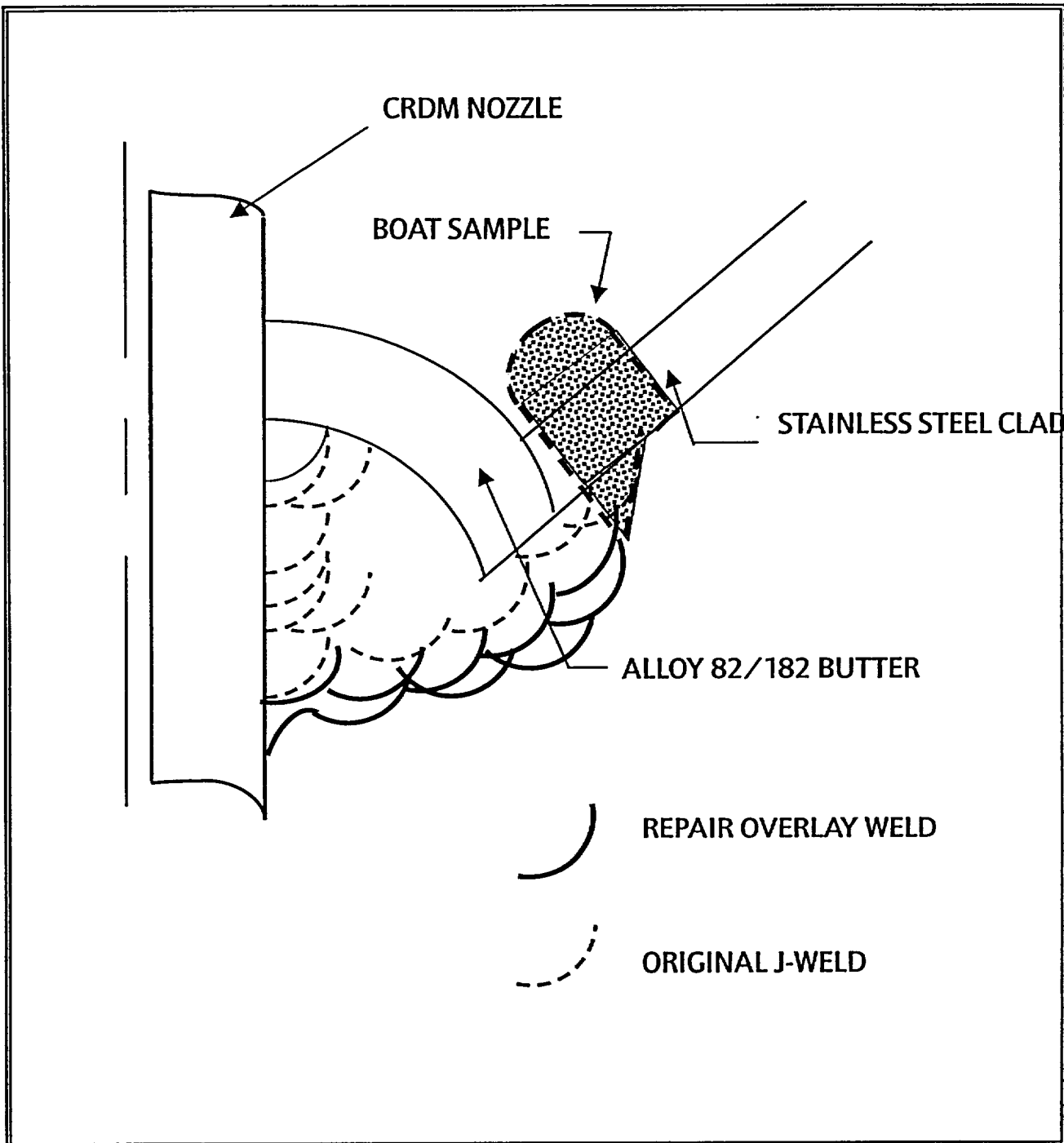


Figure B-1 Boat Sample Radial Location cut from Nozzle No. 51

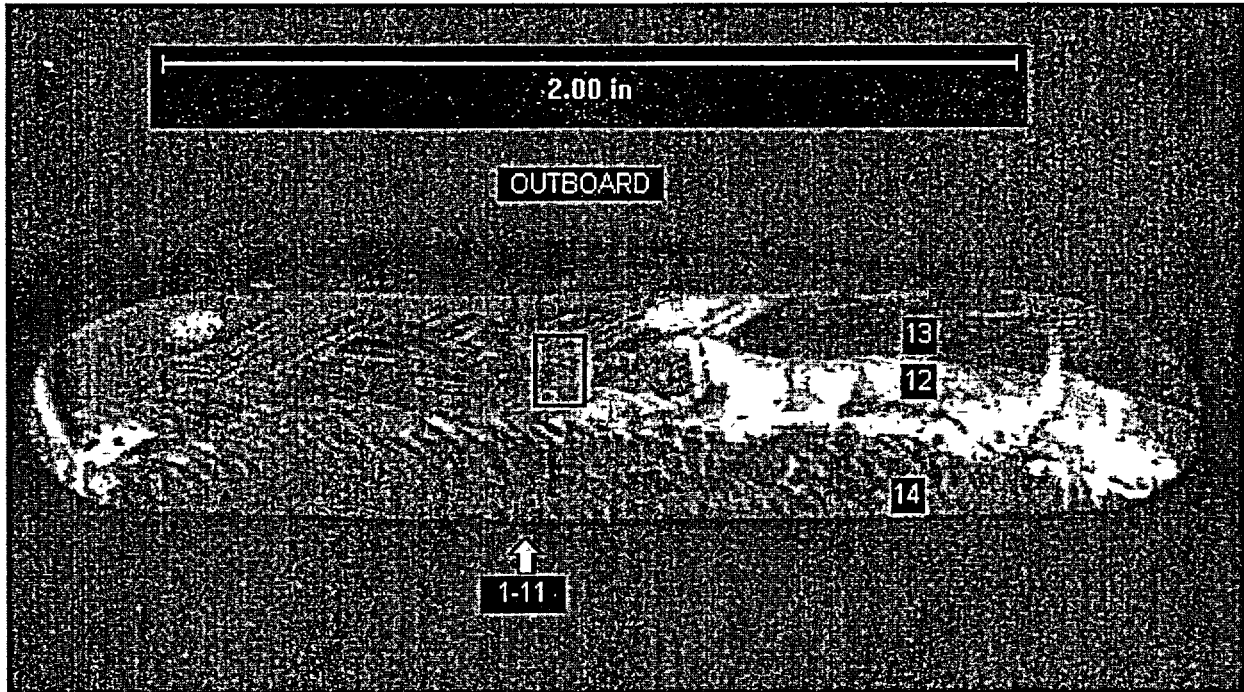


Figure B-2A As-Received Boat Sample Wetted Surface Plan View with Location of EDS Surface Analyses

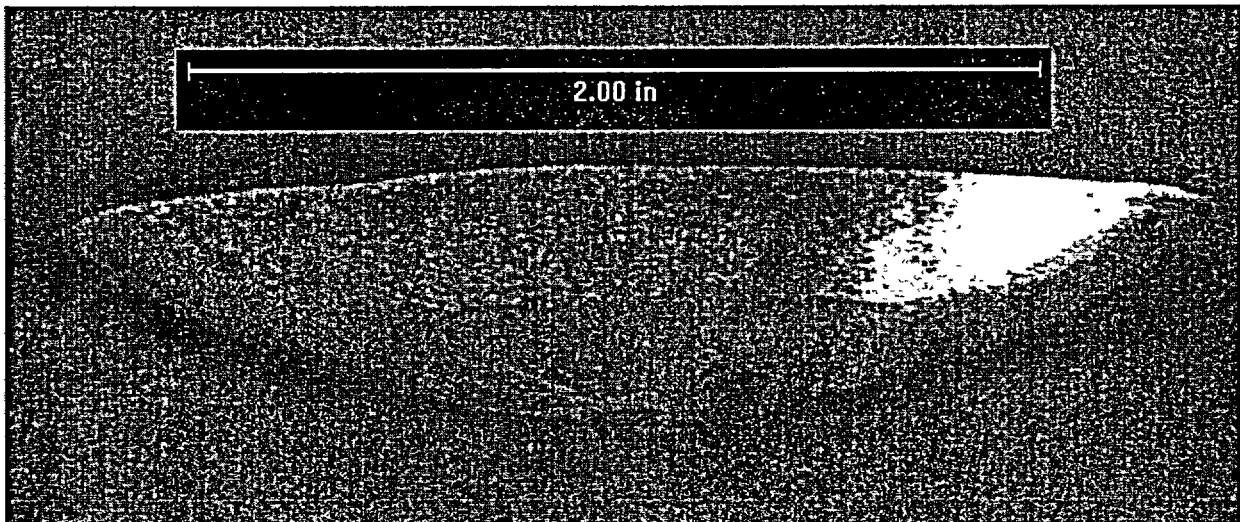


Figure B-2B As-Received Boat Sample Outboard Side View with EDM Cut Surface

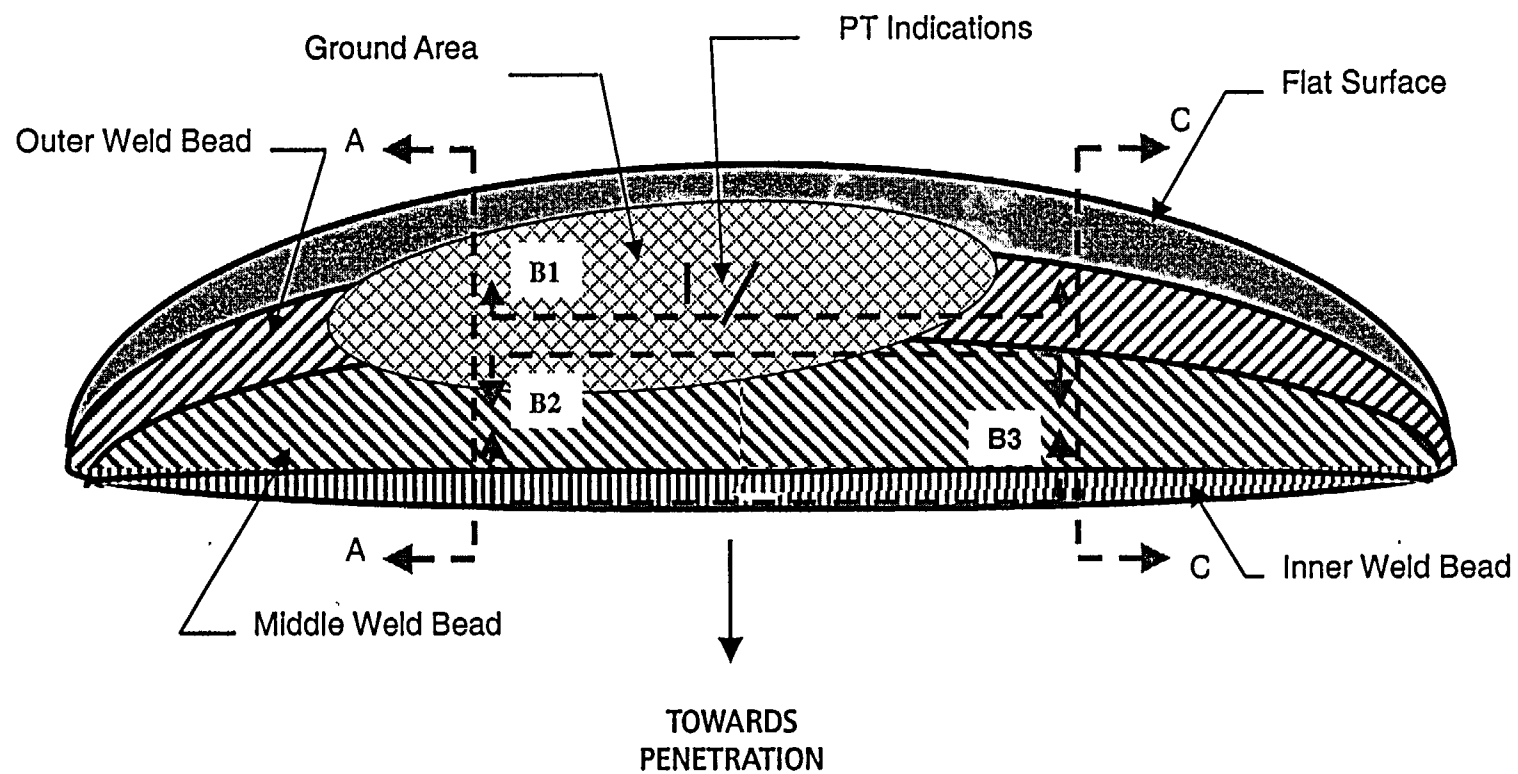


Figure B-3 Boat Sample Surface Appearance and Metallurgical Section Plan

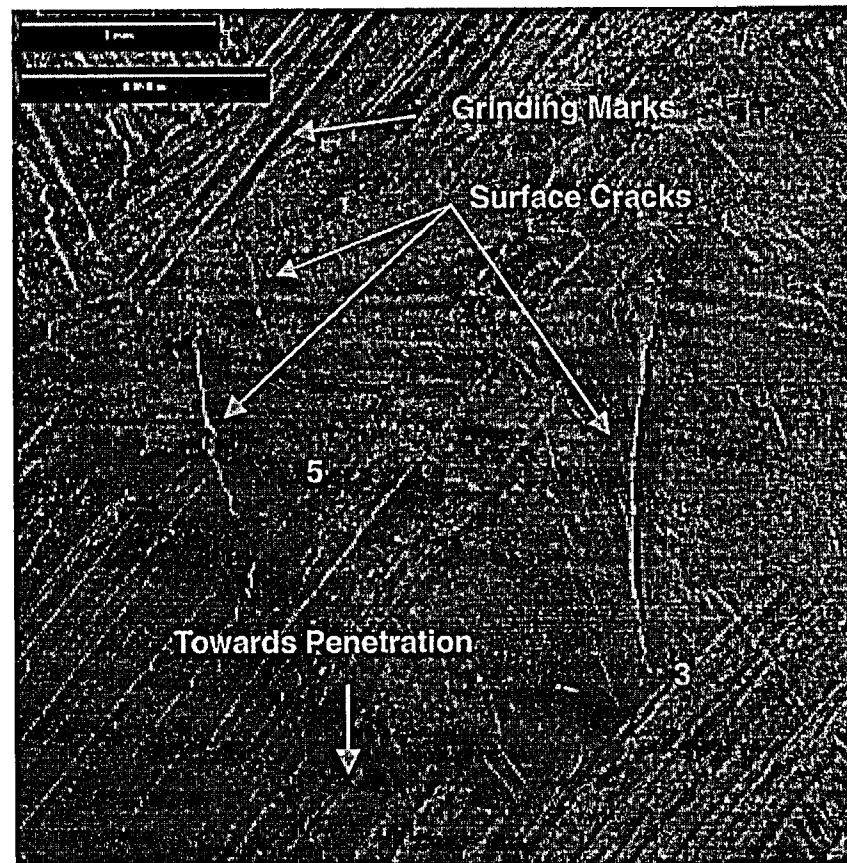


Figure B-4 Surface Cracks in Ground Area at Linear PT 135° Location

Location No.	Location Description	% Ni	% Fe	% Cr	% Al + Ti	% Nb	% Ni Dilution	% Fe Dilution	Expected % Cr	Probable Filler Metal
	308 (Nominal)	11	69	20	Not spec	Not spec				
	A-82 (Nominal)	72	2	20	< 0.75	2.5				
	A-182 (Nominal)	67	7.5	15.0	< 1.0	1.8				
	A-52(Ht.NX2424JK)	58.8	10.5	28.1	1.21	0.03				
7	Outermost Surface	9.7	64.2	18.0	0.1					308 St St
5	Near Small Crack	29.9	45.8	21.5	0.3		68	71	20.7	A-82
3	Inner Crack Tip	34.3	38.6	22.9	0.5					A-82 or 52
4	0.06" Inboard of Location 3	51.2	20.2	24.2	1.0		15	17		A-52
13	Outermost Surface	8.5	68.0	20.3	0.1					308 St St
12	Outermost Bead	51.7	23.1	21.0	0.4		32	35	20.1	A-82
14	Innermost Bead	56.7	12.9	25.4	1.6		28	24	26.6	A-52

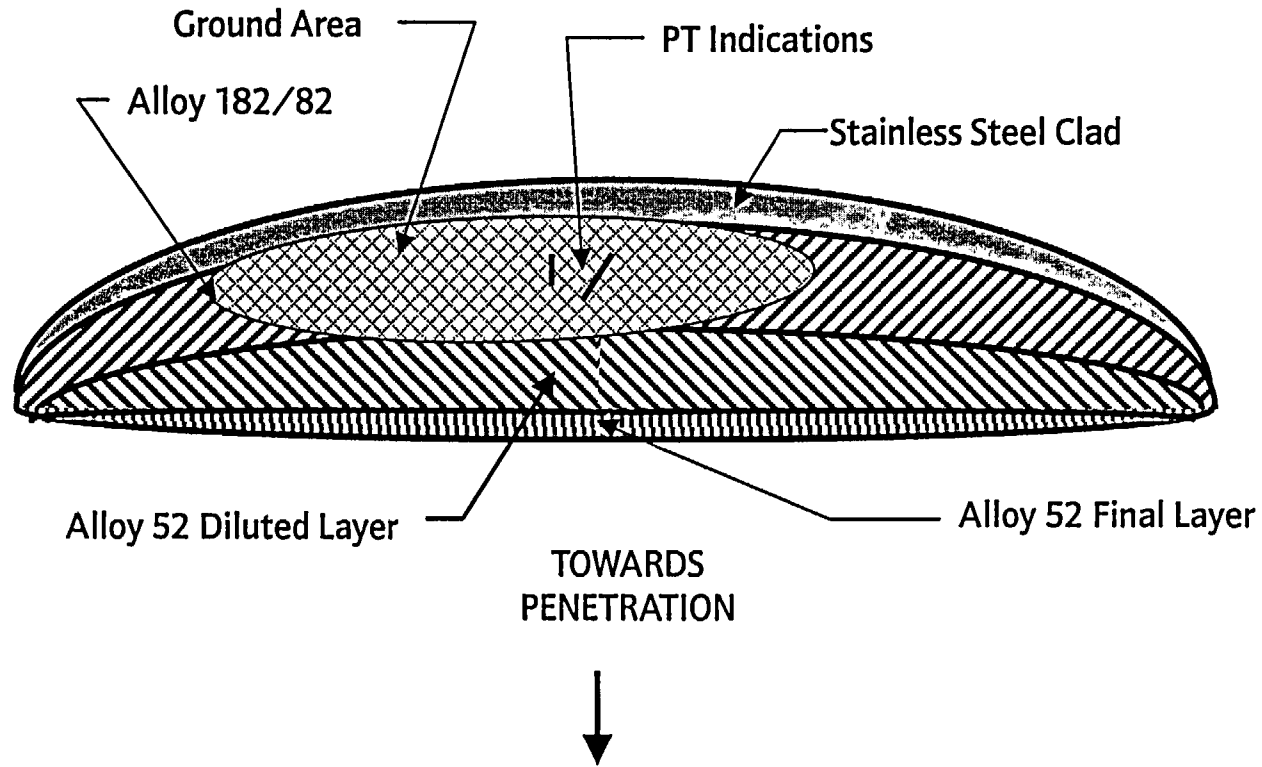
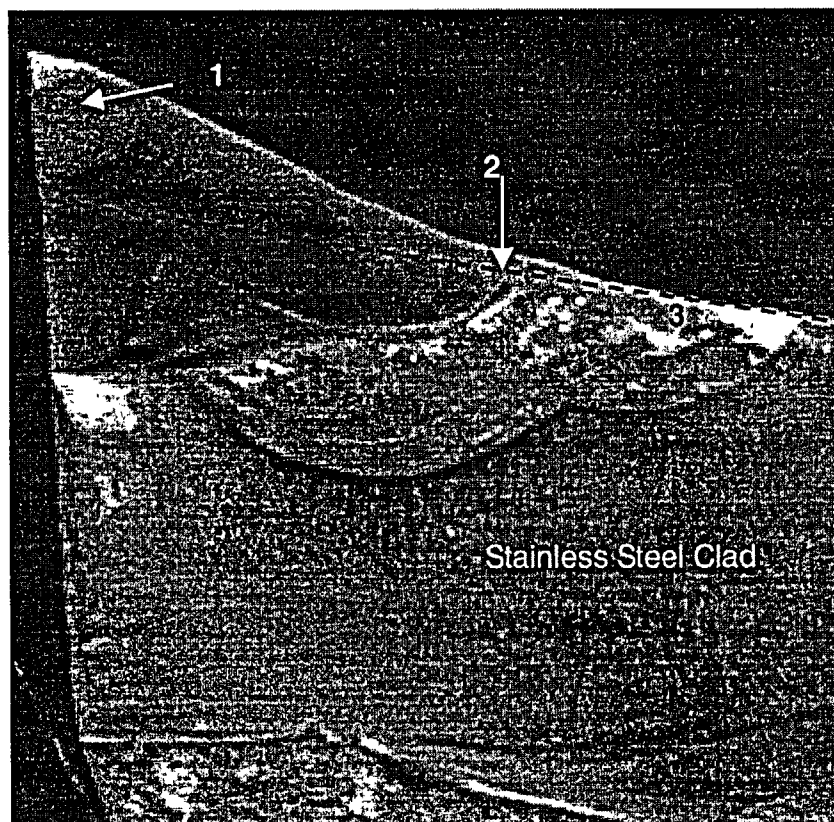
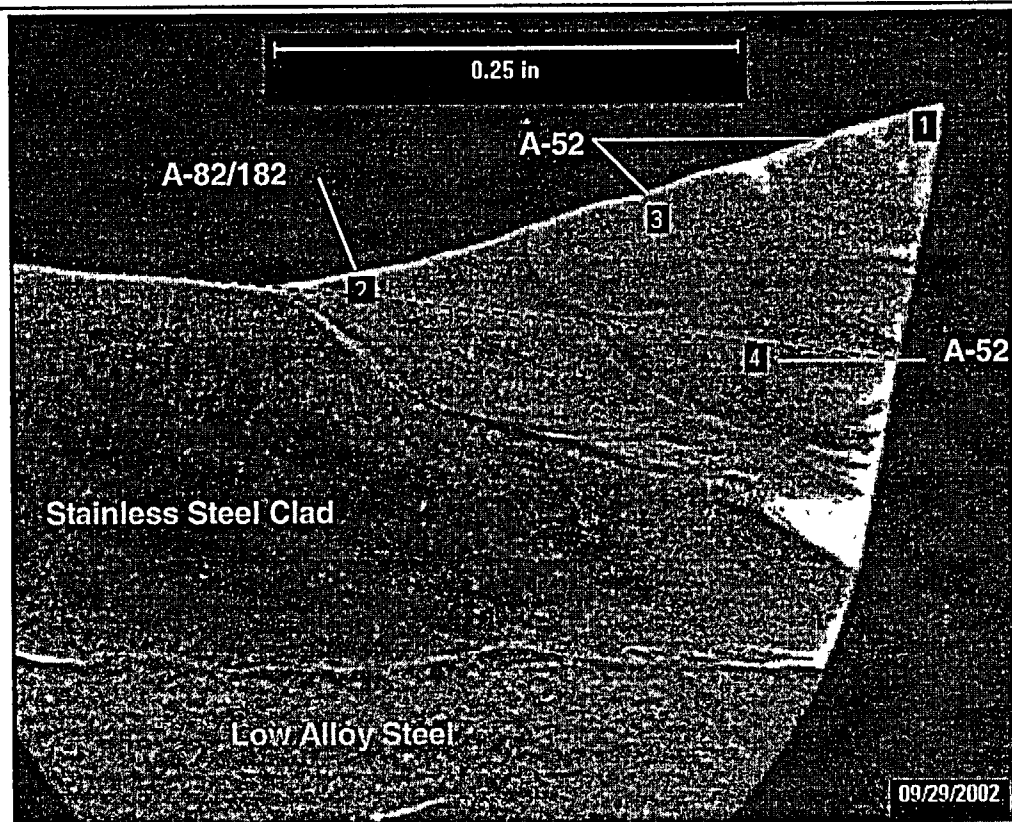


Figure B-5 Sketch of Wetted Surface Plan View with Weld Material Determination based on EDS Analysis in Table B-1



Location No.	Location	Ni	Fe	Cr	Al + Ti	Nb	% Ni Dilution	% Fe Dilution	Expected %Cr	Probable Filler Metal
1	Inboard Bead	54.8	15.7	24.9	1.2					A-52
2	Middle Bead	52.5	18.9	24.2	1.2					A-52
3	Outboard Bead	26.8	48.0	21.6	.53	0.3	65	70	20.2	A-82

Figure B-6A Metallographic Section A-A Ground Repair Weld Configuration with EDS Analyses



Location No.	Location	%Ni	%Fe	%Cr	% Al + Ti	%Nb	% Ni Dilution	% Fe Dilution	Expected %Cr	Probable Filler Metal
1	Inboard Bead	55.2	15.6	25.0	1.4	0.5				A-52
3	Middle Bead	56.8	13.6	24.4	1.2	0.5				A-52
4	Interior Bead	54.6	17.5	23.2	1.0	0.7				A-52
2	Outboard Bead	47.7	24.8	21.3	0.6	0.9	22	26	20.1	A-82

Figure B-6B Metallographic Section C-C Full Depth Repair Weld Configuration with EDS Analyses

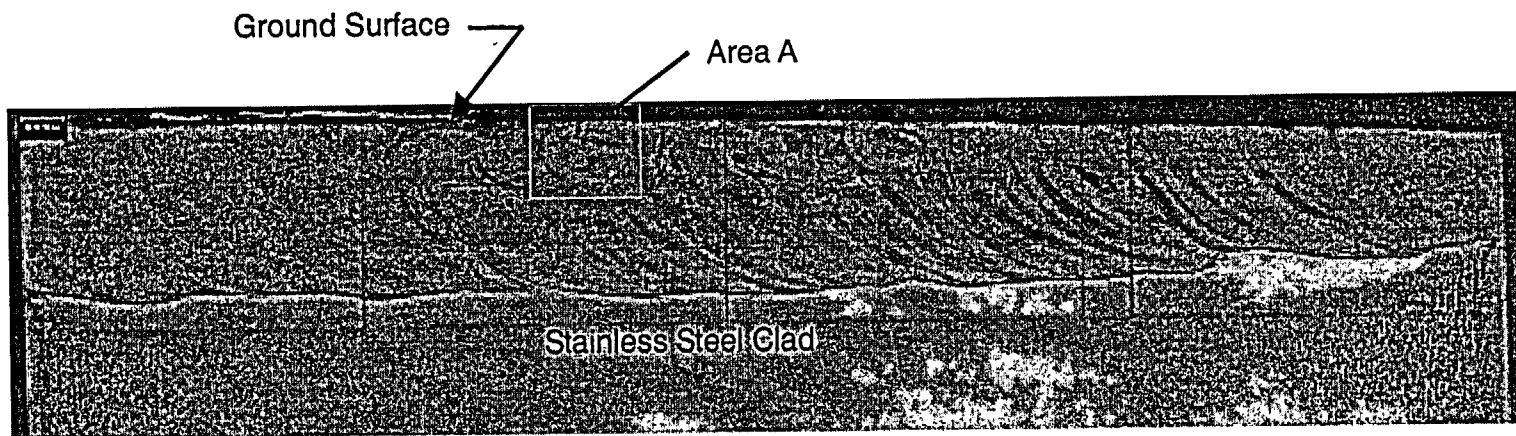
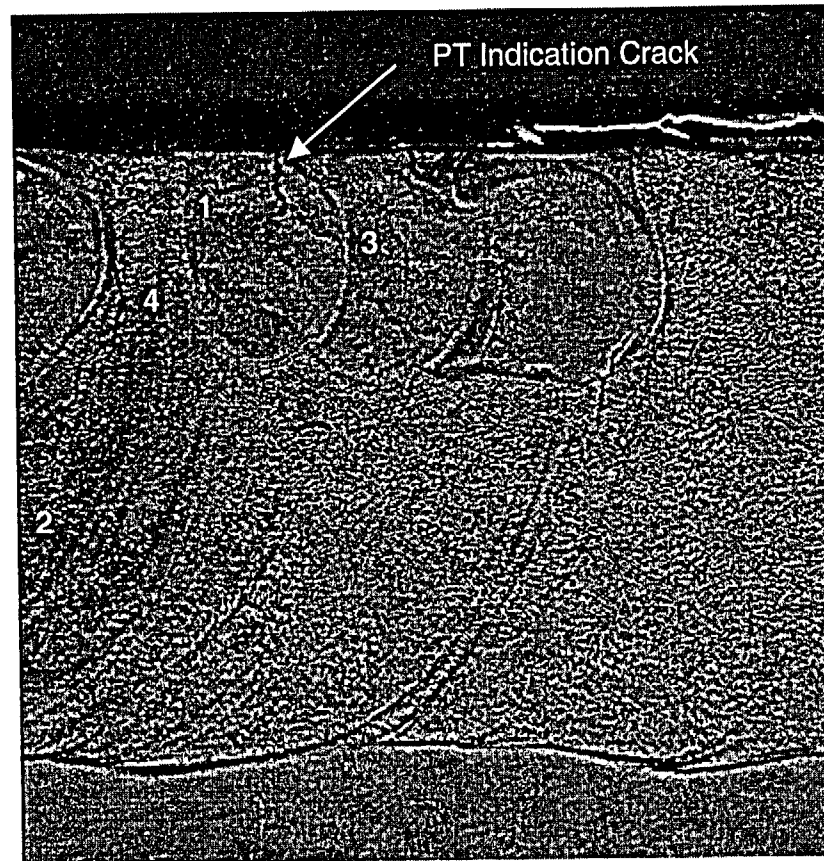


Figure B-7 Section B1 at Tip of PT Indication showing Hot Cracking at Weld Layer Interfaces



Location No.	Location	%Ni	%Fe	%Cr	% Al + Ti	%Nb	% Ni Dilution	% Fe Dilution	Expected %Cr	Probable Filler Metal
1	Intermittent Bead	40.2	31.4	22.9	0.9		62	60	24.9	A-52
3	Intermittent Bead	39.9	32.4	23.0	0.9					
2	Continuous Bead	29.0	45.5	21.7	0.4		69	69	20.2	A-82
4	Continuous Bead	29.0	45.1	21.7	0.5					

Figure B-7A Area A from Figure B-7 showing PT Indication and Other Hot Cracking with EDS Analyses

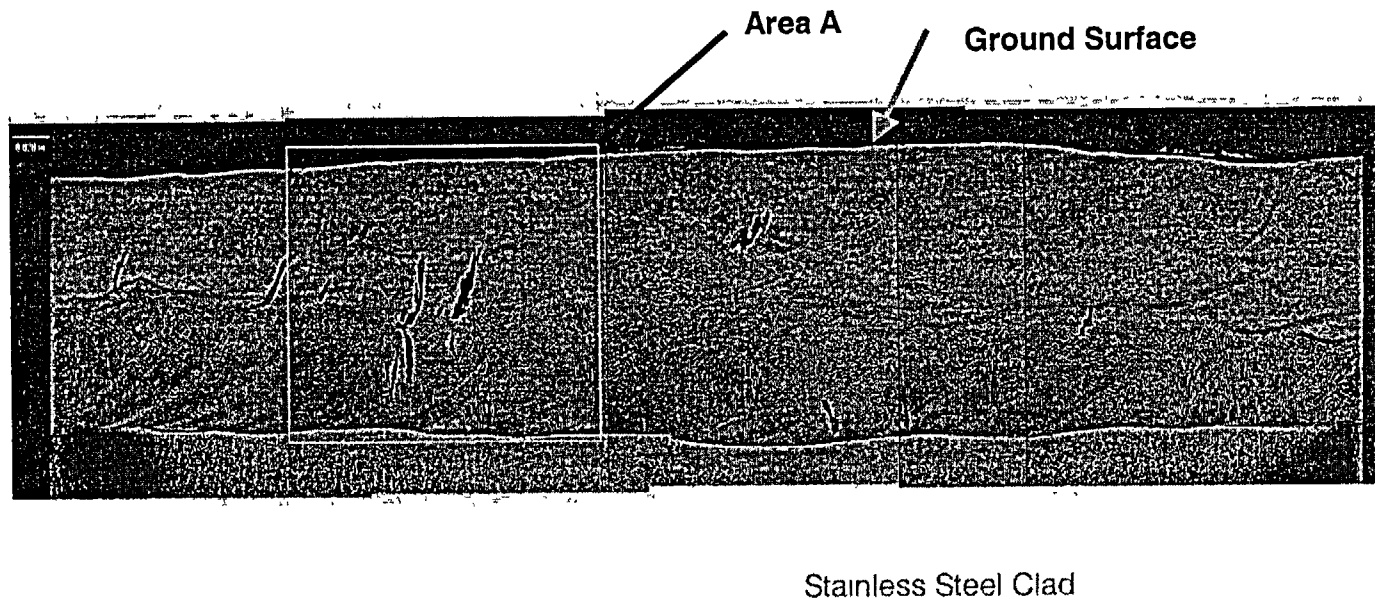
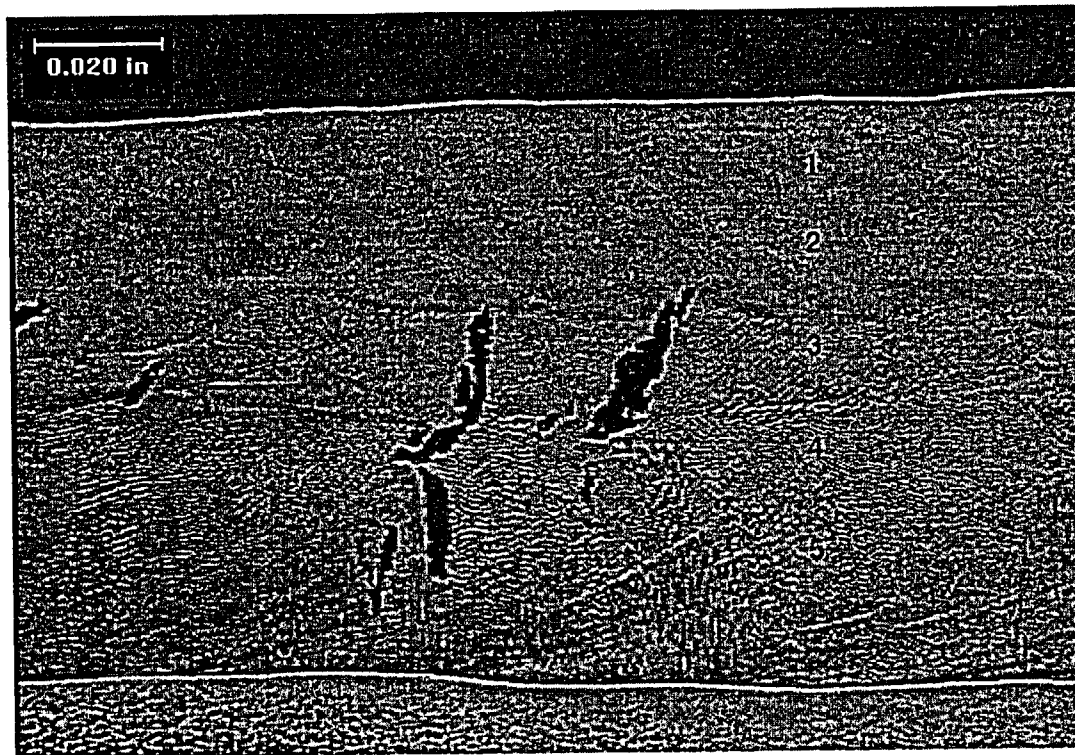


Figure B-8 Section B2 showing Hot Cracking at Weld Layer Interface



Location No.	Location	%Ni	%Fe	%Cr	% Al + Ti	%Nb	% Ni Dilution	% Fe Dilution	Expected %Cr	Probable Filler Metal
1	Top Bead	52.3	19.5	23.9	1.2	0.3	42	48	26.3	A-52
2	Top Bead	51.9	20.6	24.0	0.8	0.3				A-52
3	Middle Bead	43.2	29.2	23.5	0.8	ND				A-82 or 52
4	1 st Bead	29.5	44.4	22.1	0.5	0.3	68	69	21.4	A-82
5	1 st Bead	28.1	45.7	22.2	0.5	0.3	70	71		A-82

Figure B-8A Area A from Figure B-8 Showing Hot Cracking and EDS Analyses

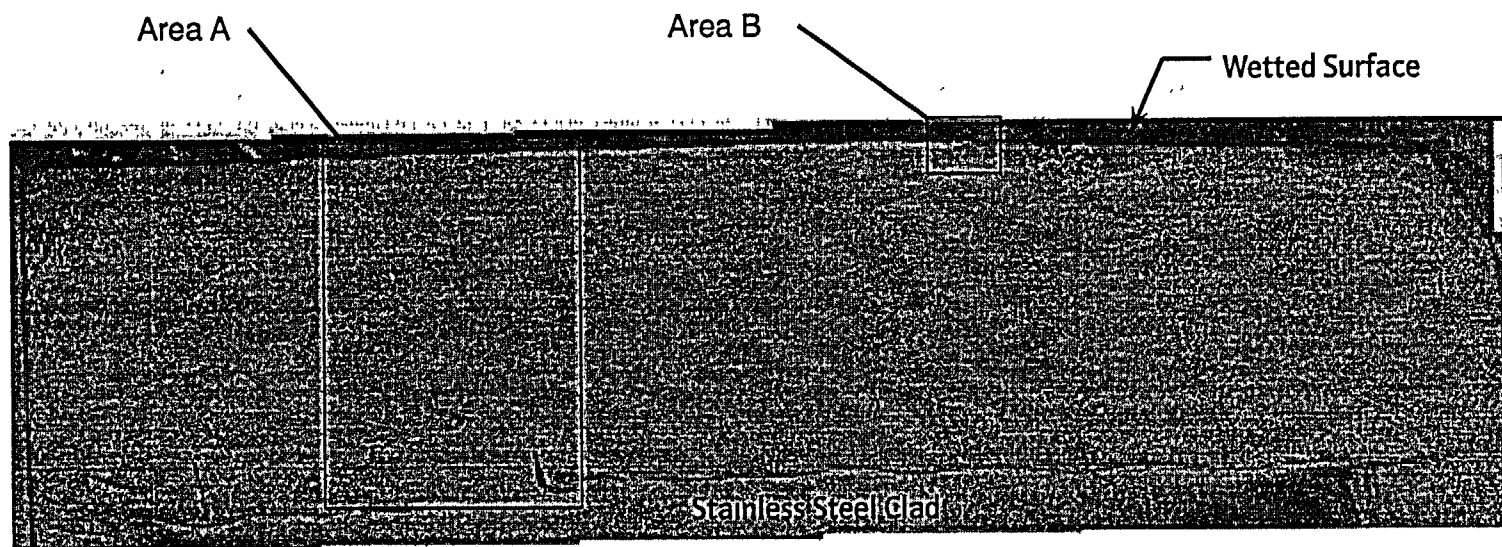
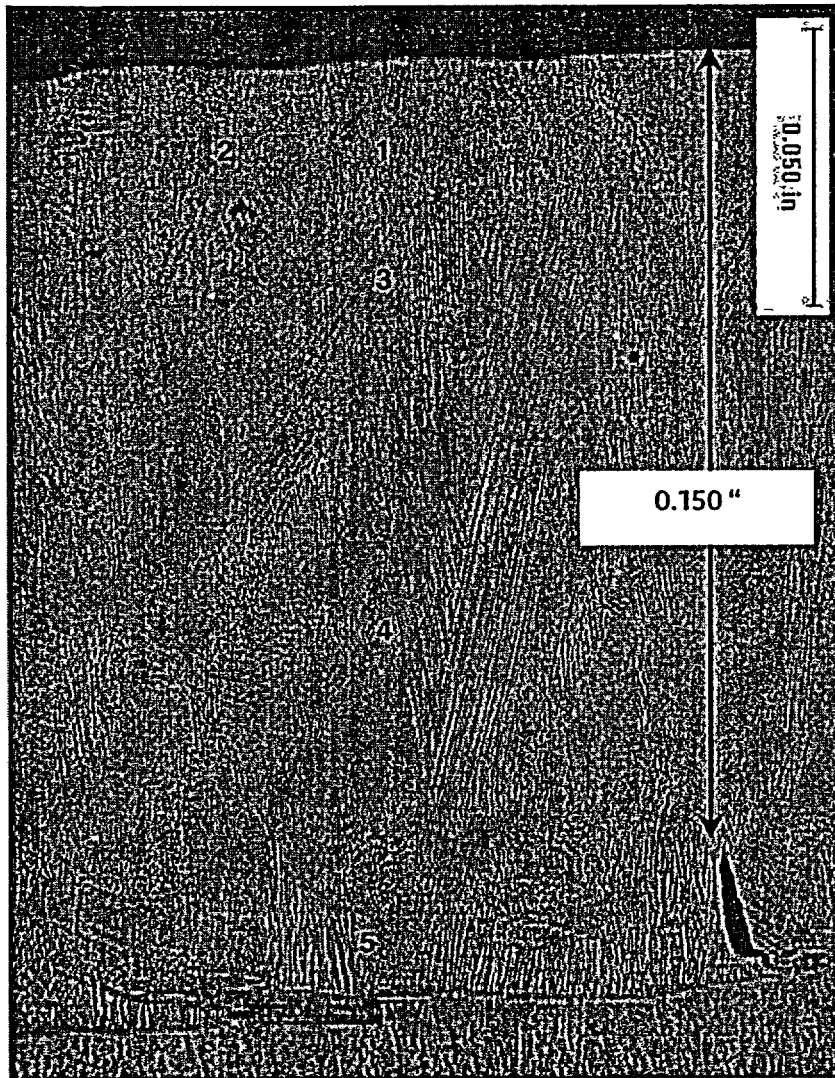


Figure B-9 Section B3 with Full Thickness Weld Repair with Minor Hot Cracking and Tungsten Inclusion



Location No.	Location	%Ni	%Fe	%Cr	% Al + Ti	%Nb	% Ni Dilution	% Fe Dilution	Expected %Cr	Probable Filler Metal
1	2 nd Repair Layer	55.4	14.4	25.2	1.6		6	8	26.3	A-52
2	2 nd Repair Layer	56.1	15.0	25.0	1.2	0.3	20	22		A-52
3	Repair Layer	55.7	15.1	25.4	1.1	ND	37	35		A-52
4	1 st Repair Layer	49.0	23.0	24.2	0.9	0.3	32	36	25.5	A-52
5	J-Weld Extension	43.3	30.2	21.7	0.7	0.3	46	46	20.1	A-82

Figure B-9A Area A from Figure B-9 showing Hot Cracking and EDS Analyses